7. Dissolved Organic Matter in Submarine Hydrothermal Systems

Susan Q. Lang

Department of Geology and Geophysics
Woods Hole Oceanographic Institution, Woods Hole, Massachusetts, USA

[NON PRINT ITEMS]

ABSTRACT

The transport and transformation of carbon in subseafloor environments is a significant component of past, present, and future global fluxes. Seawater's dissolved organic matter (DOM) enters the subseafloor and undergoes complex reactions including microbial processing, interactions with the rock matrix, and thermal restructuring and remineralization to carbon dioxide. Large shifts in concentrations, isotopic compositions, and molecular abundances provide a rich source of information about the environments through which fluids have circulated. Broad patterns linking geological settings to the fate of organic molecules can now be drawn, including the wide-scale removal of seawater DOM in ridge-flank systems, and large additions of abiotically synthesized compounds into fluids that interact with mantle rocks. Outstanding questions remain concerning the role of hydrothermal circulation as a source of refractory organic matter and its impact on the isotopic signature of deep oceanic DOM.

KEYWORDS: hydrothermal circulation, dissolved organic matter, abiotic synthesis, serpentinization, mid-ocean ridges

[Chapter Starts Here]

CONTENTS

1. Introduction

Large volumes of water have passed through the hot, rocky subseafloor of the ocean throughout Earth's history. Fluids circulate through the igneous crust to an average age of 65 Myr, creating a hydrologically active reservoir that is nearly 2% of the global volume of the ocean (Johnson and Pruis, 2003). Global mass fluxes of water passing through hydrothermal systems are on par with the export from rivers (Mottl, 2003), with the entire volume of the ocean circulating through the upper ocean crust on the order of every 100,000 – 500,000 yr (Johnson and Pruis, 2003; Fisher, 2005). Rates of hydrothermal circulation may have been higher in the geological past, when spreading rates were faster (Müller et al., 2022)

The scale of hydrothermal circulation is sufficiently large to affect the global cycling of major ions (Mg, Ca), trace metals (Fe, Mn), phosphorous, isotope systems (^{87}Sr), and the distribution of deep-sea biological communities (Wheat et al., 1996; German and Von Damm, 2003; Früh Green et al., 2022). The fate of organic compounds during passage through the oceanic crust, particularly for non-volatiles species such as amino acids, has historically received less attention. An increasing number of field studies have addressed this gap, providing insights into the physical, chemical, and biological reactions that form, remove, and alter dissolved organic matter (DOM). This information can be used to determine the role of various reactions in the global cycling of carbon and other elements including nitrogen and sulfur, to constrain the requirements for microbial life to thrive, and to identify the physical and chemical conditions that lead to the abiotic synthesis of organic compounds.

The DOM transported with seawater into the subseafloor undergoes complex reactions including microbial processing, interactions with the rock matrix, thermal restructuring, and remineralization. Hydrothermal circulation has been proposed to be responsible for: (1) 5% of the annual loss of deep ocean refractory organic carbon (Walter et al., 2018); (2) the de novo synthesis and export of organic molecules by both biological and abiotic pathways (McCollom and Seewald, 2007; Lang et al., 2010; Reeves et al., 2014; McDermott et al., 2015); (3) the stabilization of dissolved trace metals due to metal-organic complexes (Bennett et al., 2008; Sander and Koschinsky, 2011), allowing their transport across ocean basins (Tagliabue et al., 2010; Fitzsimmons et al., 2014; Resing et al., 2015); (4) water column signatures of F^{14}C dissolved organic carbon (DOC) that are anomalously low (Druffel et al., 2021); and (5) supplying dissolved aromatics to the deep sea (Dittmar and Koch, 2006; Wagner et al. 2019; Lin et al., 2019).

For the purposes of this chapter, hydrothermal circulation is defined broadly as locations where water percolates into the crust, is heated, rises buoyantly, and exits into the ocean (Fig. 7.1). The heat that drives circulation can be supplied by periodic injections of fresh magma or from lithospheric crustal cooling. Subduction zones also export fluids to the water column in conjunction with volcanic arc and back-arc systems, as do intra-plate hot spots. The fate of organic matter circulating through these heterogenous environments depends greatly on the temperature, rock type, the presence or absence of sediments, and the available reaction time.

Insert Figure 7.1

Figure 7.1: Map of known hydrothermal vent locations based on data from the InterRidge Vents Database. Modified with permission from (Früh-Green *et al.*, 2022).

II. Processes affecting organic compositions

The starting material for hydrothermal fluids is deep seawater that percolates into the crust on the downwelling, recharge limb of hydrothermal circulation systems, with additions from fluids and volatiles that degassing from magmatic inputs (Fig. 7.2). Reactions begin in the cool recharge zone and continue throughout the circulation pathway as fluids are subjected to increasing temperatures, rise buoyantly, and exit the seafloor. The final fluid composition reflects the totality of these reactions throughout the fluid pathway.

Insert Figure 7.2

Figure 7.2: General schematic of fluid flow in mafic hydrothermal systems, not to scale. Water enters the crust at recharge zones, is heated, and rises buoyantly to return to the ocean. As the crust ages and moves off axis it accumulates sediment, creating a barrier to convective fluid flow. Fluids are channeled through bare rock seamount outcrops, with active exchange with the base of the sediment column. Concentrations based on data from: Lang et al., 2006; McCarthy et al., 2010; Walter et al., 2018; Longnecker et al., 2018; Lin et al., 2019.

As elsewhere in this book, DOC is operationally defined as the material that can pass through a filter, typically with a pore size of 0.2 – 0.7 µm, remains in solution after a sample is acidified and purged to eliminate inorganic carbon, and is converted to CO_2 after high-temperature combustion, UV oxidation, or other means. Methane (CH_4) is the most abundant reduced carbon species in many hydrothermal systems, but is measured as DOC as it is too volatile to remain in solution during the purging step. Other single carbon molecules such as formate and methanol remain in solution and contribute to DOC. In this chapter, the term DOC is used when discussing the carbon in the bulk organic pool (e.g. carbon-specific analyses such as DOC concentrations and isotopes), while DOM is used to encompass the broader suite of compounds that also contain oxygen, nitrogen, and sulfur.

Downwelling seawater carries a suite of organic molecules with molecular and isotopic characteristics described in full in other chapters of this book. In brief, < 6 % of the 35 – 45 µmol L^{-1} DOC in deep seawater is characterizable at the molecular level, mostly as neutral sugars, amino acids, amino sugars, and polycyclic aromatic compounds (Benner, 2002; Repeta, 2015). During thermohaline circulation from the North Atlantic to the North Pacific, the ^{14}C age of deep seawater DOC increases from 4,000 to 6,000 ybp as concentrations decrease, while $\delta^{13}C$ signatures remain largely consistent, -22 to -19 ‰ (Druffel *et al.*, 1992; Carlson and Hansell, 2015).

Many broad-spectrum analyses that do not target specific molecular components can only be performed after salt is removed from samples by ultrafiltration, solid-phase extraction (SPE), or other means. These approaches isolate a subset of the organics (~25 – 60%) based on their molecular weight or polarity (see Chapter 2 by Repeta and Aluwihare for review). Suites of structurally related carboxyl-rich alicyclic molecules (CRAM) and acylated polysaccharide carbohydrates are major components of the organic matter isolated in these ways, identifiable as broad peaks by Nuclear Magnetic Resonance (NMR) spectroscopy (Aluwihare et al., 1997; Hertkorn *et al.*, 2006). Analysis by Fourier Transform Ion Cyclotron Resonance Mass Spectrometry (FT-ICR-MS) demonstrates the presence of several thousand unique masses, each of which may be a mixture of isomers (Kujawinski *et al.*, 2009). In this section, the processes that transform, remove, and add to this initial deep seawater organic pool are described (Fig. 7.3).

Insert Figure 7.3

Figure 7.3: Organic transformations in the rocky subseafloor. As seawater percolates into the crust, DOC interacts with the rock matrix and is altered by microbial processing, thermal reordering, remineralization, and input of abiotic molecules.

A. Thermal transformation and degradation – The seminal finding that chlorophyll degradation products were present in crude oil and coal (Treibs, 1936) was foundational to the field of organic geochemistry (Kvenvolden, 2006). The recognition that biologically synthesized molecules could be transformed into more stable, long-lived geomolecules gave rise to innumerable studies on the transformation and degradation pathways of organic compounds under elevated temperatures and pressures. Some of this information can be generalized to predict and understand the fate of organics due to thermal reworking. Further studies designed specifically to mimic hydrothermal conditions in controlled laboratory settings and field observations provide additional insights.

Chemical bonds break in the order of their relative strength, starting with the non-covalent bonds that sorb organics onto mineral surfaces, followed by bonds involving heteroatoms (oxygen, sulfur, nitrogen) and, finally, carbon-carbon bonds (Tissot and Welte, 1984). At temperatures below ~80°C microbial degradation, dehydration (removal of water), oxidation, and other low-temperature reactions break down macromolecules (Tissot and Welte, 1984; Shock, 1993; Shock et al., 2019). Due to the presence of water, oxygenated degradation products are favored such as carboxylic acids, alcohols, ketones, in addition to alkenes and hydrocarbons. (Eglinton et al., 1987; Seewald, 2001a; Shock et al., 2019). Major products that are generated upon heating sediments or seawater organics include acetate, carbon dioxide (CO_2), and CH_4 (Kawamura *et al.*, 1986; Wellsbury *et al.*, 1997; Zhuang *et al.*, 2019; Hawkes *et al.*, 2016; Lin et al., 2017). Laboratory experiments indicate n-alkanes are oxidized to carboxylic acids, short-chain hydrocarbons, CO_2 and CH_4 through a series of stepwise oxidation reactions (Fig. 7.4; Seewald et al., 2001a; 2001b; 2006).

Figure 7.4: Reaction pathways during the stepwise oxidation of aqueous n-alkanes to carboxylic acids, short chain hydrocarbons, CO_2, and CH_4, as proposed by Seewald, 2001a; 2001b; 2003

Insert Figure 7.4

At temperature ranges of 150-250°C, organic matter deamination (removal of an amino group to release NH_3) and decarboxylation (removal of a carboxyl group to release CO_2) occur (Seewald et al., 1990; Hunt, 1979; Qian *et al.*, 1993). Oxygen- and nitrogen-bearing compounds can undergo substitution reactions that transform their functional groups (Shock et al., 2019; Robinson et al., 2020). Hydration reactions are favored at lower temperatures, while dehydration is increasingly favored as temperatures increase (Shock *et al.*, 2013). Oxidation and reduction reactions are also common, and potentially reversible (Seewald et al., 1994; Shock et al., 2013).

At very high temperatures (>~300°C), organics undergo reduction, condensation (loss of water to form a new carbon-carbon bond), and dehydration reactions to form macromolecules and aromatics, causing compounds to revert to their most stable state (Simoneit, 1985; Didyk and Simoneit, 1989). Therefore, in addition to the complete remineralization of organic matter into CO_2, stable molecules such as cyclic and aromatic structures are also formed, as well as condensates and insoluble organic carbon, some of which can persist at temperatures >300°C (Eglinton et al., 1987; McCollom et al., 2001; Rushdi and Simoneit, 2004; Hawkes *et al.*, 2016). The favored reaction products at equilibrium are CO_2, CH_4, and graphite. As a consequence, the concentrations of DOC are lower after seawater is exposed to elevated temperatures, and the molecules that remain in solution are have lower molecular weight, and have lower O/C ratios as insoluble condensates remain in the solid phase (Lin *et al.*, 2017; Hawkes *et al.*, 2016; Rossel *et al.*, 2017; Longnecker *et al.*, 2018).

The outcomes of laboratory experiments must be interpreted with some caution as situ conditions are not always well replicated. For instance, in some experiments designed to simulate hydrothermal conditions, oxygen was not eliminated from the system, and mineral buffers that would modulate pH and redox conditions were not included. The reactions that molecular species undergo may therefore differ from those in natural systems (Shock, 1992). Redox state, pH, and the presence of H_2 are particularly influential on the fate of organic molecules (Shock et al., 2019; Glein et al., 2020; Robinson et al., 2021), and both parameters are strongly impacted by mineral buffering (Shock and Schulte, 1998; Shock *et al.*, 2013; Johnson-Finn et al., 2020, 2021).

B. Microbial processes – The regions of the crust and mantle that are hydrologically active host a diverse array of bacteria, archaea, eukaryotes, and viruses (Orcutt *et al.*, 2011; Anderson et al., 2013; Hu *et al.*, 2021). Analogous to processes that control DOM cycling in the surface ocean, biological autotrophic and heterotrophic activities also impact the DOM pool within the rocky subsurface. Thus, the organic signatures of autotrophy, heterotrophy, and degradation of biomass that have been developed to understand carbon cycling in the water column and sediments, such as lipid biomarker isotopes and amino acid degradation indices, can also be used to track similar processes in hydrothermal systems (Pearson et al., 2005; Bradley, Hayes and Summons, 2009; Lang *et al.*, 2013; Lin *et al.*, 2015).

Chemosynthetic microorganisms utilize geochemical energy with metabolisms such as methanogenesis, methanotrophy, sulfate reduction, sulfide oxidation, and hydrogenotrophy (Summit and Baross, 2001; Schrenk et al., 2010; Orcutt *et al.*, 2011; Reveillaud et al., 2016; Dick, 2019). Autotrophs flourish in the dynamic regions where hydrothermal fluids carrying reduced chemical species (H_2, CH_4, H_2S, Fe^{2+}) mix with oxygenated seawater and provide the most thermodynamic energy, such as in hydrothermal plumes and diffuse fluids (Amend and Shock, 1998; McCollom and Shock, 1997; McCollom, 2000; Amend and Shock, 2001; Amend *et al.*, 2011). In contrast, increasing evidence indicates that heterotrophic organisms dominate microbial populations in the ocean crust away from active mixing zones (Mason *et al.*, 2010; Li *et al.*, 2020; Suzuki *et al.*, 2020).

C. Abiotic synthesis – One of the most surprising findings of the past several decades is the recognition of wide-spread abiotic synthesis of organic molecules in hydrothermal settings. Many of the synthesized compounds, such as CH_4 and short-chain hydrocarbons (McCollom and Seewald, 2007; Proskurowski *et al.*, 2008), are too volatile to contribute to the operationally defined DOC pool. But the abiotic synthesis of the single carbon organic acid formate has now been demonstrated in multiple ultramafic-influenced systems in micro-molar to milli-molar concentrations (Lang *et al.*, 2010; McDermott *et al.*, 2015; Eickenbusch *et al.*, 2019), and does contribute to DOC. Methanethiol (CH_3SH) has been identified at trace concentrations in many types of hydrothermal fluids (Reeves et al., 2014). Laboratory experiments suggest that amino acids can be produced abiotically in hydrothermal environments (Oro *et al.*, 1959; Hennet et al., 1992; Yanagawa and Kobayashi, 1992; Aubrey, Cleaves and Bada, 2009). While tryptophan and structurally similar organic molecules have been proposed to be present deep subseafloor rock cores (Menez *et al.*, 2018), amino acids identified in hydrothermal fluids to date have been attributed to biological processes (Lang *et al.*, 2013; Lin *et al.*, 2015; Svensson et al., 2004).

D. Sorption and organomineral interactions – In sediments and soils, organic matter is tightly bound with iron-bearing mineral phases, particularly iron oxides, causing its long-term preservation (Keil *et al.*, 1994; Hedges and Keil, 1995; Kaiser and Guggenberger, 2000; Lalonde *et al.*, 2012; Coward et al., 2018; Moore et al., 2023). Mineral surfaces in general, and iron oxides in particular, are widespread in the mafic and ultramafic subseafloor. Clays are a primary alteration product (Giggenbach, 1984; Frost and Beard, 2007; Yamashita *et al.*, 2019;), providing extensive surfaces for organic sorption and organomineral interactions. To date, the role of sorption for controlling the fate of organic molecules during hydrothermal circulation is largely unexplored.

III. Isotopic changes to DOM during hydrothermal circulation

Stable carbon ($\delta^{13}C$) and radiocarbon ($F^{14}C$) signatures are powerful tracers of the reactions that form and remove organic molecules, and of carbon sources. The $\delta^{13}C$ values reflect fractionation processes that differ across anabolic and metabolic pathways (e.g. Gelwicks et al., 1994; House et al., 2003; Nguyen et al., 2020), abiotic synthesis pathways (McCollom and Seewald, 2001), and degradative pathways (e.g. Penning and Conrad, 2006). The numerous processes that impact $\delta^{13}C$ values can make them interpretation complicated. $F^{14}C$ (or $\Delta^{14}C$) values are corrected for isotopic fractionation processes using $^{13}C/^{12}C$ isotopic ratios, and therefore reflect only carbon sources and radioactive decay. New ^{14}C molecules are formed in the atmosphere and quickly enter surficial inorganic and organic carbon pools ($F^{14}C \approx 1$). In contrast, mantle and ancient carbon present in the subseafloor lack ^{14}C ($F^{14}C \approx 0$). Radiocarbon analysis can therefore be a powerful tool for tracking sources of carbon in hydrothermal systems due to the large dynamic range of potential carbon sources and its independence from complicating fractionation effects.

The isotopic signature of bulk DOC from hydrothermal settings has only been reported for a few locations to date, primarily in mafic ridge flank and diffuse systems (McCarthy *et al.*, 2011; Walter *et al.*, 2018; Lin *et al.*, 2019). In conjunction with decreases in concentration, the $F^{14}C$ and $\delta^{13}C$ of the DOC are also more depleted compared to seawater signatures (Fig. 7.5). Radioactive decay during long circulation times is too minor to account for the depletion, and cannot account for changes in $\delta^{13}C$ values. Chemosynthetic microorganisms that utilize ^{14}C-depleted inorganic carbon will synthesize organic matter with depleted $F^{14}C$ and distinct $\delta^{13}C$ values and could account for the observed data (McCarthy *et al.*, 2011; Lang *et al.*, 2018). At the Juan de Fuca ridge flank, however, there are strong indications of selective removal of isotopically enriched DOC, leaving the remaining organic pool depleted in ^{13}C and ^{14}C, and would also lead to these signatures (Lin *et al.*, 2019). Whether a similar mechanism is widespread and can account for the general observation of depleted organics in mafic hydrothermal systems remain an open question.

***Insert Figure 7.5 ***

Figure 7.5. $F^{14}C$ and $\delta^{13}C$ of DOC from mafic diffuse vents and ridge flank systems vs. DOC concentrations. Data sources: Juan de Fuca fluids (JdFR; McCarthy et al., 2010; Lin et al., 2019); North Pond fluids (Walter et al., 2015); seawater (these papers and Druffel et al., 1992, 2016, 2021).

Ultramafic systems will fundamentally differ from mafic regimes, although the bulk isotopic signatures of DOC from ultramafic systems have not yet been reported. DOC concentrations are higher than deep seawater (Lang et al., 2010; 2018), primarily due to abundant abiotically synthesized formate that can reach concentrations of hundreds of $\mu mol\ L^{-1}$ (Lang *et al.*, 2018; McDermott *et al.*, 2015). The isotopic signatures of formate have been reported at one hydrothermal field and are $F^{14}C$ 0.09 – 0.56, depending on the input of locally mixed seawater dissolved inorganic carbon (DIC) into the fluids (Lang *et al.*, 2018). Whether seawater DOC is removed during circulation to a similar extent as in mafic systems is unknown, as elevated bulk DOC concentrations would mask its loss. It is likely that ultramafic systems, in general, export $F^{14}C$ depleted organics.

IV. Concentrations and compositions of hydrothermal DOM

Early studies regarded hydrothermal systems as the outcome of reactions between two relatively uniform materials, hot oceanic crust, and seawater. In reality, a wide diversity of rock types, magmatic degassing, temperatures, extent of biological activity, mixing dynamics, and episodic events give rise to a large number of diverse systems, each with unique geochemical characteristics. The attempt to broadly categorize the organic signatures of hydrothermal system types below draws inferences from scarce and at times conflicting data, and likely oversimplifies the diversity of systems that exist.

A. High-temperature mafic black smoker type systems – Ongoing magmatic inputs at fast and intermediate mid-ocean ridge spreading centers create new oceanic mafic ocean crust consisting of gabbros and basalts. Quintessential black smoker systems are hosted on this young (<0.1 Ma) crust and discharge fluids to temperatures >400°C (Fig. 7.2). One of the earliest studies on the organic geochemistry of hydrothermal fluids demonstrated that the concentrations of amino acids in black smoker fluids were lower compared to surrounding seawater, making it one of the earliest demonstrations of organic removal during hydrothermal circulation (Haberstroh and Karl, 1989).

The bulk concentrations of DOC in high-temperature fluids from sediment-free mafic vent fields on the Juan de Fuca Ridge (8 – 26 µM; Lang *et al.*, 2006; Hawkes *et al.*, 2015) and the East Pacific Rise (8.5 µmol L^{-1}; Longnecker *et al.*, 2018) are less than one-third seawater concentrations (~36 µmol L^{-1}). Low Mg fluids indicative of minimal seawater entrainment during sampling from the E2 field in the Southern Ocean are reported to have DOC concentrations both lower and higher than seawater (34 – 52 µmol L^{-1}), as are samples from Menez Gwen (6 – 215 µmol L^{-1}) (Hawkes *et al.*, 2015). The cause of these high and variable bulk DOC concentrations are unclear, but issues with contamination during sampling cannot be ruled out given the extreme technical challenges of sampling high-temperature fluids. In addition to the loss of bulk DOC, the portion of dissolved organic compounds that SPE can isolate decreases with Mg concentrations in mafic high-temperature systems, suggesting that the CRAM and carbohydrate components that contribute to SPE are removed (Hawkes *et al.*, 2015). Based on the low DOC values, the annual removal of DOC due to high-temperature hydrothermal circulation is estimated to be approximately 10^9 mol C yr^{-1} (Lang et al., 2006; Table 7.1).

A diverse suite of compounds has been identified in high-temperature fluids (300 – 370°C) along the Mid-Atlantic ridge. Concentrations of n-alkanes and n-fatty acids were generally in the 0.1 – 12 ppb range at the TAG, Snake Pit, Menez Gwen, and Lucky Strike sites, while mono- and poly-aromatic hydrocarbons were present at concentrations in sub-ppb levels (Konn *et al.*, 2022). At TAG and Snake Pit, low concentrations of formate (1 – 2 µmol L^{-1}) and acetate (2 – 8 µmol L^{-1}) were detected (Konn *et al.*, 2022). Dissolved n-alkanes have also been identified in hot fluids from the East Pacific Rise at concentrations of ~2 µg L^{-1}, along with derivatives of benzoic acid and a hump in the analytical spectrum that reflects the presence of an unresolved complex mixture (UCM) of compounds (Longnecker *et al.*, 2018).

Table 7.1. Representative characteristics of different types of hydrothermal systems where data is available. Numerous system types have not yet been sufficiently characterized to provide flux estimates.

	Representative Values				
System type	**Temp (°C)**	**pH**	**DOC[a] (µmol L^{-1})**	**Fluid flux[b] (10^{16} g yr $^{-1}$)**	**Net DOC flux[c] (mol C yr^{-1})**
Mafic, axial systems (0 - 1 Ma)					
High temperature	300 - 400°C	2 - 5	8 - 26	3 - 6	**–** 10^9
Diffuse	5 - 100°C	4 - 7	35 - 70	280 - 560	**+** 10^9 to 10^{10}
Mafic, off axis systems (1 - 65 Ma)					
Ridge flank, warm	≥45 °C	7.5	12 - 16	7 - 43	**–** 10^9 to 10^{10}
Ridge flank, cool	5 - 45 °C	7.5	18 - 30	4,800	**–** 10^{11}
Ultramafic, with minimal magmatic input	40 - 120 °C	9 - 11	70 - 100	poorly constrained	
Deep Seawater (>1500 m)	2 - 5 °C	7.8	36 - 45		

[a] DOC concentrations and fluxes from (Lang *et al.*, 2006; Lang *et al.*, 2010; Walter *et al.*, 2018; Longnecker *et al.*, 2018; Lin et al., 2019). Negative values indicate a net removal of DOC from the ocean during circulation while positive values indicate a net gain.

[b] Fluid flux from (Elderfield and Schultz, 1996; Mottl, 2003; Johnson and Pruis, 2003)

[c] Net DOC flux from (Lang *et al.*, 2006; Walter *et al.*, 2018). Negative values represent a net loss of seawater DOC during circulation

B. On Axis Diffuse Fluids – Diffuse venting occurs adjacent to the focused flow of high-temperature vents, where seawater enters the crust locally and mixes with hydrothermal fluids (Fig. 7.2; Bemis, Lowell and Farough, 2012). Low-temperature fluids can also be generated by reactions with warm rock, in the absence of a high-temperature fluid input. Heat flux studies indicate that the fluid flux through diffuse vents may be as high as 10x greater than through high temperature focused flow (Schultz et al., 1992; Veirs et al., 2006; Elderfield and Schultz, 1996) (Table 7.1). Axial diffuse vent fluids often are subseafloor mixing zones between hydrothermal fluids that carry reduced chemical species (H_2, CH_4, H_2S, Fe^{2+}) and seawater that carries oxidized chemical species (O_2, NO_3^-, SO_4^{2-}), making them ideal locations for chemosynthetic microorganisms (Summit and Baross, 2001; Huber et al., 2003; Dick, 2019). Metabolisms such as oxidation of H_2, methanogenesis, methanotrophy, and sulfate reduction are thermodynamically favorable and can support extensive primary production (McCollom, 2000; Amend *et al.*, 2011; Dick, 2019). In many diffuse vent fluids, concentrations of CH_4 are higher than expected from a conservative mixing between seawater and pure hydrothermal fluids, while H_2 and H_2S concentrations are lower, likely as the result of subseafloor biological activity (Von Damm and Lilley, 2004; Wankel *et al.*, 2011).

While the amount of biomass that chemosynthetic processes in mixing zones can support is a small fraction of the photosynthetic biomass (McCollom, 2000), these biological hotspots may have local impacts and can help support dense invertebrate biomass (Le Bris *et al.*, 2019). The organic matter produced in diffuse fluids is a likely source for the ligands and macromolecules that complex with iron and other metals (Sander and Koschinsky, 2011; Lough *et al.*, 2019), allowing their transport across ocean basins (Tagliabue *et al.*, 2010; Fitzsimmons, Boyle and Jenkins, 2014; Resing *et al.*, 2015).

Diffuse fluids have DOC concentrations higher than local deep seawater, which has been attributed to biological synthesis in the subseafloor (Lang *et al.*, 2006; McCarthy *et al.*, 2011; Rossel *et al.*, 2015; Longnecker *et al.*, 2018). The $\delta^{13}C$ values of this DOC from the Juan de Fuca Ridge are slightly more positive than near-by deep seawater (-18.5 vs. -21.1‰), while the $F^{14}C$ values that are lower ($F^{14}C$ of 0.5157 vs 0.5600), also possibly reflecting local primary production that incorporates inorganic carbon containing less ^{14}C than seawater DIC (McCarthy et al., 2011). Water-soluble vitamins, amino acids, and organic sulfur compounds have been identified in diffuse fluids, albeit at sub-micromolar concentrations (Longnecker *et al.*, 2018).

C. Ridge flank systems – As the oceanic crust ages and moves away from the ridge crest, water continues to advect through the permeable rocky oceanic crust and lithosphere to ages of 65 Ma (Fig. 7.2; Stein and Stein, 1994; Johnson and Prius, 2002). Substantial sedimentary cover hinders the hydraulic connection between bottom water and the basement, so most circulation on the older crust is channeled through topographic seafloor highs such as seamounts (Fisher and Wheat, 2010).

Ridge flank circulation that occurs at relatively cool temperatures (10-20°C) has the largest fluid fluxes of any type of known hydrothermal systems, estimated to be 4,800 x 10^{16} g seawater yr^{-1} (Mottl and Wheat, 1994; Johnson and Pruis, 2003). Example systems include the Dorado outcrop offshore from Costa Rica on 23Ma crust (Wheat and Fisher, 2008) and the North Pond system on 7–8 Ma crust on the western flank of the Mid-Atlantic Ridge (Edwards et al., 2012; Villinger *et al.*, 2019).

Due to the lower temperatures, the inorganic geochemistry of the fluids is often nearly indistinguishable from seawater (Wheat *et al.*, 2019). Nonetheless, substantial losses of DOM have been documented in cool ridge flank fluids, with concentrations as low as one-third of seawater values (18 – 30 µmol L^{-1}), leading to an estimated annual removal of 10^{11} mol of DOC, or 5% of the global annual DOC loss (Walter *et al.*, 2018).

Larger DOC concentration losses are observed in the warmer ridge flank systems that occur where thick sediment layers provide thermal insulation, such as on the Juan de Fuca Ridge flank (Fig. 2). Due to smaller water fluxes, the global annual removal of DOC is at least an order of magnitude lower than in cool ridge flank systems (Table 7.1). Fluid temperatures of 65°C and residence times of hundreds to thousands of years (Elderfield *et al.*, 1999; Mottl *et al.*, 1998), and diffusive exchange with overlying sediments, cause more significant geochemical changes to the fluids (Wheat *et al.*, 2013; Mottl and Wheat, 1994). Up to 75% of seawater organics are removed from the system, resulting in concentrations of 12 – 16 µmol L^{-1} (Lang *et al.*, 2006; Lin *et al.*, 2012). Despite the large net loss of seawater organics, NMR data suggests seawater CRAM remains in the fluids, and aromatics are added, with $\delta^{13}C$ values only slightly more negative than local seawater (Lin *et al.*, 2019). Free amino acids (1 – 13 nmol L^{-1}) and dissolved hydrolysable amino acids (43-89 nmol L^{-1}) are present in the fluids with distributions indicating they are degraded, possibly due to *in situ* biological production and/or inputs from porewaters from the overlying sediments (Lin *et al.*, 2015).

D. Ultramafic systems – Slow and ultra-slow spreading centers occur where plate spreading is not associated with robust injections of fresh magma and constitutes approximately 50% of global mid-ocean ridges. Lower crustal and upper mantle rocks are exhumed through tectonic controls. These ultramafic rocks undergo substantially different water-rock reactions when exposed to seawater. Alteration reactions associated with the hydration of olivine and orthopyroxene, called serpentinization, create fluids that contain abundant H_2 as a by-product of the reaction and tend to be more alkaline at low temperatures than purely mafic systems. High CH_4 concentrations are also characteristic, as the H_2 reacts with mantle or seawater inorganic carbon to form CH_4 through Fischer-Tropsch-type reactions (McCollom and Seewald, 2007).

Systems with little to no magmatic input, such as the Lost City field, host moderate temperature fluids (< 115°C) that are high pH (9 – 11), with concentrations of H_2 and CH_4 that reach 15 mmol kg^{-1} and 2 mmol/kg respectively (Kelley *et al.*, 2005). The Rainbow field has a significant magmatic component (Canales *et al.*, 2017), resulting in high temperature fluids (365°C) with low pH (2.8), but a clear ultramafic influence in the form of abundant H_2 (16 mmol/kg) and CH_4 (2.5 mmol kg^{-1}) (Charlou *et al.*, 2002). The Von Damm has no obvious magmatic input but features that are a mixture of these endmembers, with fluids that reach maximum temperatures of 226°C, a pH of 5.6, and high H_2 and CH_4 concentrations (18.2 and 2.8 mmol L^{-1}) (McDermott *et al.*, 2015).

The abundant H_2 in ultramafic systems provides the thermodynamic drive for the formation of organic molecules, both biologically and abiotically (Shock *et al.*, 2013). The energy available for chemosynthetic metabolisms is higher in the mixing zones from ultramafic fields than mafic fields (McCollom, 2007; Amend *et al.*, 2011; Reveillaud *et al.*, 2016), though this does not necessarily translate directly to higher cell counts or activities as other factors may limit life (Lang and Brazelton, 2020). Biologically synthesized amino acids (1 – 2 µmol L^{-1}) and fatty acids (1 – 6 µmol L^{-1}), reach concentrations comparable to productive coastal surface waters (Lang *et al.*, 2013; McCollom et al., 2015). Acetate has also been identified in µmol L^{-1} concentrations, likely due to the degradation of biomass (Lang *et al.*, 2010). Other suites of molecules that would be expected to form as the result of primary production, such as neutral sugars and amino sugars, have not yet been analyzed but are also likely present due to abundant biological activity.

The high H_2 concentrations also lead directly to the abiotic formation of the single-carbon organic acid formate. At Lost City, formate concentrations reach 158 µmol L^{-1} while they are up to 669 µmol L^{-1} at the Von Damm site (Lang *et al.*, 2010; McDermott *et al.*, 2015). The higher formate concentrations at Von Damm are due in part to higher initial DIC concentrations. DIC concentrations at Lost City are vanishingly low (<1 µmol L^{-1}) due to carbonate precipitation in the subseafloor, which causes carbon limitation in the fluids (Bradley et al., 2009; Lang *et al.*, 2018).

While no published data on the ^{14}C content of bulk DOC in ultramafic systems yet exists, it is likely that depleted ^{14}C signatures accompany the very high total DOC concentrations. In the Lost City fluids that are most representative of subseafloor conditions, more than 50% of the carbon pool is formate, which is strongly depleted in ^{14}C ($F^{14}C$ of 0.09) and enriched in ^{13}C ($\delta^{13}C$ of -12.1 ‰; Lang et al., 2018). Fatty acids are also a significant portion of the dissolved carbon pool (15%), and are also highly enriched in ^{13}C ($\delta^{13}C$ of -7.6 to -3.6‰; Konn et al., 2009; McCollom et al., 2015). The fatty acids are likely mobilized from bacterial biomass in the chimneys or subseafloor (Konn *et al.*, 2009; McCollom et al., 2015), where similar compounds have $F^{14}C$ signatures of 0.13 (Lang *et al.*, 2018). The widespread depleted ^{14}C signatures in abiotic and biological molecules reflect the incorporation of ^{14}C-free mantle carbon, and lead to the export of organics with depleted ^{14}C signatures into the water column.

E. Sedimented systems – When spreading centers and volcanic hotspots are adjacent to continents with high sedimentation rates, heated fluids may pass through organic-rich sediments, transforming and mobilizing organic molecules. Smaller and more aqueous soluble compounds are preferentially carried in fluids such as smaller alkanes (< C_{10}), oligopeptides, oligosaccharides, compounds containing C-N-S bonds, and aromatic volatiles (Simoneit, 1985; Kawka and Simoneit, 1987). Acetate and other organic acids are some of the most abundant soluble degradation products (Kawamura *et al.*, 1986; Seewald, 2001a, b; Shebl and Surdam, 1996; Lundegard and Kharaka, 1994; Fisher, 1987; Eglinton et al., 1987). Reactive amino acids, polysaccharides, and small peptides are also released (Lin *et al.*, 2017). As a result, the residual organics retained in the sediments are often enriched in compounds that have undergone condensation reactions, as well as other reactions that make them less soluble (Kvenvolden and Simoneit, 1990; Kawka and Simoneit, 1987; Simoneit et al., 1988; Simoneit and Fetzer, 1996; Rushdi and Simoneit, 2004).

Lower temperature pore fluids from heated sediments at Guaymas basin contain high DOC concentrations (up to 8.8 mmol L^{-1}), but these concentrations decrease as fluids reach temperatures >100°C (Lin *et al.*, 2017; Zhuang *et al.*, 2019). Pore fluids also contain abundant acetate (up to 229 µmol L^{-1}) and other low molecular weight compounds including formate (6 – 9 µmol L^{-1}), lactate, methanol (0.2 – 37 µmol L^{-1}), and ethanol (0.6-15 µmol L^{-1}), due to biologically mediated degradation of sedimentary organic matter (McKay *et al.*, 2012; Teske *et al.*, 2016; Zhuang *et al.*, 2019). Hydrolysable amino acids reach concentrations of 5 µM (Lin *et al.*, 2017). Fluids from the sedimented hydrothermal field Middle Valley on the Juan de Fuca Ridge contain short chain hydrocarbons (C_2H_4 to C_4H_{10}, <1 to 236 µmol L^{-1}), as well as elevated abundances of benzene (1 – 28 µmol L^{-1}) and toluene (0.1 – 6 µmol L^{-1}) (Cruse et al., 2006).

F. Hotspots, Volcanic Arc, and Back-arc systems – Intra-plate volcanism is caused when magmatic plumes originating from the mantle ascend and create hotspots. Known hydrothermal circulation associated with these hotspots is generally low temperature (<50°C) (Michard *et al.*, 1993; Staudigel *et al.*, 2004; Glazer and Rouxel, 2009), but sufficiently extensive to be traced in the water column across ocean basins (Jenkins *et al.*, 2020). Iron and manganese oxidation have the potential to fuel extensive chemosynthetic microbial biomass (Emerson and Moyer, 2002; Edwards, Bach and McCollom, 2005).

Hydrothermally active submarine arc and back-arc regions are created at the subduction zones of convergent plate boundaries. Subducting oceanic plates form magmas that are rich in volatiles (Wallace, 2005; Plank *et al.*, 2013), and give rise to submarine volcanoes that host acidic fluids with high CO_2, SO_2, and trace metal concentrations (de Ronde and Stucker, 2015).

At this time, data from fluids associated with volcanic settings are too heterogenous to draw broad inferences on the fate of carbon during circulation. Diffuse vents sampled from the back-arc system West Matta at the NE Lau Basin contained DOC concentrations that were similarly high (39 – 521 µmol L-1) to diffuse vents on spreading centers due to biological synthesis of organics (Lin *et al.*, 2021). In contrast, shallow submarine vents associated with the Aeolian archipelago and with volcanic islands east of Taiwan host low temperature fluids with DOC concentrations similar to or substantially lower than local seawater (Svensson, Skoog and Amend, 2004; Yang *et al.*, 2017). High yields of total dissolved neutral aldoses in one vent fluid suggests the associated organics may be labile (Svensson, Skoog and Amend, 2004) while minimal uptake during incubation experiments with a different vent fluid suggests limited bioavailability (Yang *et al.*, 2017).

The fore-arc region of subduction zones gives rise to low-chlorinity springs due to the dewatering of the subducting slab (Fryer, 2012). Springs hosted on the Mariana fore-arc form from subducted slab fluids passing through mantle rocks on the overlying slab, inducing serpentinization (Fryer, 2012). The springs and the pore fluids associated with the resulting mud volcanoes have high concentrations of DOC, formate, and acetate, due to the combined influences of degrading sediments, microbial activity, and abiotic synthesis (Mottl *et al.*, 2004; Haggerty and Fisher, 1992; Eickenbusch *et al.*, 2019; Mottl *et al.*, 2023).

G. Hydrothermal Plumes – The warm, buoyant fluids that exit the seafloor rise into the water column and are diluted with seawater (~1:1000) to create nonbuoyant plumes that disperse from vent sites with oceanic currents (German and Von Damm, 2003; German and Seyfried, 2015). The chemical disequilibria created by mixing chemically reduced fluids with oxygenated seawater creates metabolic energy to fuel primary productivity, so long as abiotic oxidation of geochemical species is kinetically hindered (McCollom, 2000). Plumes host microbial communities that mediate the oxidation of CH_4, NH_4^+, Mn, Fe, and reduced S compounds (Winn et al., 1986, Kadko et al., 1990; De Angeles et al., 1993; Lam et al., 2011; Anantharaman et al., 2016). Elevated concentrations of particulate organic carbon (POC) with distinct $\delta^{13}C$ values are widely observed in hydrothermal plumes of all types, often in conjunction with higher DOC concentrations (Bennett et al., 2008; 2011; Lam et al., 2008; Breier et al., 2012; Lin et al., 2021). The elevated organics could be entrained from the biological biomass, inhabiting diffuse fluids, the walls of high-temperature chimneys, or from in situ carbon fixation within the plume. Organic aggregates are intimately associated with minerals, and appear to be composed of protein-rich biomolecules, exopolymer-like matrices, organic ligands, and microorganisms (Toner et al., 2009; Breier et al., 2012). Complexes with organic compounds stabilize dissolved trace metals, allowing their dispersal far from local vent fields (Bennett et al., 2008; Toner et al., 2009; Sander and Koschinsky, 2011).

V. Potential impacts on the molecular composition of seawater DOM

Transport of seawater through hydrothermal systems is both a net source and sink of marine DOM, broadly dependent on the type of system (Table 7.1). The majority of organic matter in deep seawater is removed during circulation through mafic high-temperature systems and ridge flank systems, while organics are added to diffuse fluids, sedimented systems, and ultramafic-influenced systems (Table 7.1). Beyond net fluxes, organic molecules' reactions during circulation through the crust may also influence the distributions of molecules in the deep sea.

CRAM and carbohydrates are major components of deep seawater DOM (Aluwihare et al., 1997; Hertkorn *et al.*, 2006; Arakawa *et al.*, 2017). Their fate during hydrothermal circulation is difficult to assess as only a small number of studies have applied the techniques used to identify these molecules in seawater, such as NMR, to hydrothermal fluids. One exception is a detailed study of low-DOC ridge flank fluids that demonstrated that CRAM remains present in the fluids, and is only partially decomposed and removed during circulation (Lin *et al.*, 2019). Similarly, despite net losses in DOC concentrations, CRAM-like material is still present in high-temperature fluids from the East Pacific Rise (Longnecker *et al.*, 2018).

Hydrothermal vents have been implicated as potential sources for thermogenic black carbon and aromatic compounds to the abyssal ocean (Dittmar and Koch, 2006; Yamashita *et al.*, 2022). A diverse suite of polyaromatic hydrocarbons (PAHs) and benzene polycarboxylic acids (BPCAs) have been identified in the deep ocean waters (Dittmar and Koch, 2006; Yamashita *et al.*, 2022), with ^{13}C and ^{14}C isotopic signatures distinct from riverine sources, making oceanic inputs likely (Ziolkowski and Druffel, 2010; Wagner *et al.*, 2019). Concentrations of aromatic compounds and graphite are elevated in fluids from mafic high-temperature vents on the EPR (Estes *et al.*, 2019), Menez Gwen (Rossel *et al.*, 2017), and Rainbow (Konn *et al.*, 2009), Lucky Strike (McCollom et al., 2015), the ultramafic Lost City system (Konn *et al.*, 2009), the Juan de Fuca ridge flank (Lin *et al.*, 2019), as well as in sedimented systems in the Guaymas Basin (Simoneit, 1985) and Middle Valley on the Juan de Fuca Ridge (Cruse and Seewald, 2006).

Most focus has been on high-temperature mafic vents as the potential primary sources of aromatics to the deep sea. When reported, concentrations of aromatics are low in high-temperature fluids, in the nano-molar or pico-molar level for high-temperature vents on the EPR and Mid-Atlantic Ridge (Longnecker *et al.*, 2018; Konn *et al.*, 2022). The approaches used to detect aromatics differ across studies, and the absence of detection may simply reflect that the compounds were of a structural type outside the analytical window. Nonetheless, the fluid fluxes through high-temperature mafic systems are relatively small, and total DOC concentrations are relatively low, in comparison to other types of hydrothermal circulation (Table 7.1).

In contrast, fluxes through diffuse and ridge flank systems are substantially larger and heating studies suggest that some aromatic compounds may form over hours to days even at temperatures as low as 55°C (Rossel *et al.*, 2015; Rossel *et al.*, 2017). Aromatics are elevated over deep seawater abundances in ridge flank systems despite a large net loss of bulk DOC concentrations (Lin *et al.*, 2019).

Sedimented hydrothermal systems are an additional alternative potential source of aromatics. Black smoker fluids from sedimented Middle Valley contain benzene (28 µmol L^{-1}) and toluene (6 µmol L^{-1}), translating into a total of 210 µmol C L^{-1} (Cruse and Seewald, 2006). Their concentrations are unquestionably higher than what could be present in sediment-free black smoker or ridge flank systems, where *total* DOC concentrations are typically <20 µmol C L^{-1}. Total fluid fluxes through sedimented systems are poorly constrained, making it difficult to extrapolate to global contributions. Exports of total DOC solely from the Guaymas Basin system, however, are estimated as ~10^9 mol C yr^{-1} (Lin *et al.*, 2017), on par with global estimates of DOC from all mafic, sediment-free, black smoker systems (Table 7.1; Lang *et al.*, 2006).

VI. Impacts likely differ across ocean basins

The fate of organic matter during hydrothermal circulation depends in part on the volcanic and tectonic regimes that host circulating fluids (Table 7.1). Therefore, the geographical distribution of vent field types is important to acknowledge when considering the impact of hydrothermal circulation on the deep marine DOC cycle. The fast and ultra-fast spreading centers that form new ocean crust and give rise to high-temperature black smoker type systems are largely located in the Pacific Ocean (German et al., in press). In contrast, the mid-Atlantic Ridge is slow-spreading with more input from ultramafic water-rock reactions (German et al., in press).

The fast-spreading East Pacific Rise (EPR, 20°S 115°W) may have an outsized influence on deep ocean geochemistry. The southern section of this ridge is the fastest known spreading center in the world. Signatures of its vent fluids have been observed across the Pacific Ocean (Lupton and Craig, 1981), and dissolved iron, manganese, and aluminum exported from the EPR can be detected thousands of kilometers from the source (Fitzsimmons, Boyle and Jenkins, 2014; Resing *et al.*, 2015).

The EPR may similarly impact the regional deep DOC pool. Water column samples collected near the EPR contained DOC with unusually low $\Delta^{14}C$ and $\delta^{13}C$ signatures in locations previously shown to have elevated concentrations of excess 3-helium ($^3He_{ex}$), a conservative hydrothermal tracer (Druffel *et al.*, 2021). Similar to other mafic vent fields, high-temperature fluids on the EPR contain only 8.5 µmol L^{-1} of DOC, less than one-third of local seawater concentrations of 44 µmol L^{-1}, while low-temperature diffuse fluids contain 46 µmol L^{-1} (Longnecker *et al.*, 2018). While the isotopic signatures of bulk organic matter have not yet been determined at the EPR, data from other mafic environments suggests it will be significantly depleted in ^{14}C compared to seawater (Fig. 7.5) and could be responsible for the water column depleted isotopic signatures of DOC observed by Druffel et al., (2021).

The Pacific Ocean hosts multiple sedimented hydrothermal systems as numerous spreading centers and volcanic hot spots occur adjacent to continental settings, including the Guaymas Basin in the Gulf of California (Simoneit and Lonsdale, 1982), Middle Valley on the Juan de Fuca Ridge, near Northwestern U.S. (Cruse and Seewald, 2006), and Escanaba Trough on the Gorda Ridge, off the coast of northern California (Gieskes *et al.*, 2002). The organic content of fluids passing through sediments is quite high (see Section III.E), but water fluxes of these systems are not well constrained, making their influence on the deep ocean DOC cycle unclear.

The western Pacific is populated by arc and back-arc systems associated with subduction zones. Intra-plate volcanism creates hotspots that are also predominantly located in the central and western Pacific

Ocean. As discussed in Section III.F, the data available for these types of systems is sparse and heterogenous, and hampers predictions of their global influence.

The Atlantic Ocean hosts the slow-spreading Mid-Atlantic Ridge, while ultraslow spreading centers are found primarily in the Arctic and the Southwest Indian Ridge, with a short segment on the Mid-Cayman Rise. Concentrations of DOC in low and moderate-temperature ultramafic settings are substantially higher than in deep seawater, and much of this material is likely depleted in $F^{14}C$ compared to seawater (see Section III.D). The influence on the isotopic composition of deep DOC will, therefore, likely differ significantly from systems in the Pacific Ocean.

VII. Major unknowns

A. Broad spatial and temporal patterns – Fully integrating the geochemical fluxes associated with hydrothermal circulation into DOM cycles is challenging because of their heterogeneity in space and time. It is now clear that the fate of organics differs substantially based on the geological setting of circulation. But only a small number of systems, such as those on the Juan de Fuca ridge flank and the Lost City vent field, have been characterized for their organic signatures multiple times and by more than one research group. Most vent fields – or even types of systems – have only been sampled once. Significant gaps remain on the fate of organics in multiple system types, and whether unexpected signatures from some locations are robust or are due to sampling artefacts.

Large geochemical perturbations occur regularly with tectonic-volcanic events such as earthquakes, magmatic injections, and even tidal pressure fluctuations (see Rubin *et al.*, 2012 for review). Most of what is known on hydrothermal systems' organic geochemistry results from samples collected at single time points. The long-term stability of the organic component of hydrothermal systems is largely unknown, as is the impact of large but brief events such as underwater eruptions. Identifying these patterns can inform models of the global exchange of carbon between the ocean and lithosphere, which may have been greater in the geological past when spreading rates were higher due to the breakup of Pangaea (Müller et al., 2022).

B. Direct access to the rocky subseafloor – The life that inhabits the mixing zones in the near subseafloor substantially alters the DOM signatures and can obscure the alterations that have occurred earlier in fluid flow pathways. Efforts to sample from boreholes drilled directly into the rock subseafloor have the potential to bypass this biological overprinting, and identify transformations that occur in the deeper, hotter crust.

C. Robust, targeted experimental insights – Experimental efforts to recreate hydrothermal conditions in laboratory settings effectively demonstrated the abiotic synthesis of organic molecules (see McCollom and Seewald, 2007 and Shock et al., 2019 for reviews). Reaction progress will change with conditions such as pH, redox state, water-rock ratios, pressure, and even the reactivity of vessel surfaces containing the experiment. Isotope labels and tracking mass balances can be used to ensure that newly formed products are from the expected starting material and not organics introduced extraneously. These types of approaches have been applied quite successfully to track the fate of individual and suites of compounds, but have not yet been deployed as extensively to understand the fate of complex organic matter in seawater.

D. Source and sink of refractory DOM – The refractory organic matter carried with seawater is removed to different extents during hydrothermal circulation, depending on the geological setting. New material can be added, leading to fluids that have similar bulk concentrations but distinct isotopic and molecular composition. The organic constituents exported from these settings remain poorly constrained in most cases. As a result, it remains an open question of how the biotic and abiotic modification that DOM undergoes impacts its bioavailability, and whether hydrothermal systems are responsible for major refractory components of the oceanic DOM reservoir.

VIII. Acknowledgements

This manuscript benefited from ongoing discussions with colleagues including Jeffrey Seewald, Tom McCollom, Gretchen Früh Green, William Brazelton, Geoff Wheat, and Karyn Rodgers. An early draft was greatly improved by recommendations from Maddie Petersen, Jessica Rodgers, Jeffrey Seewald, Everett Shock, Tom McCollom, and Huei-Ting Lin. Natalie Renier (WHOI) helped create Figure 3. Support was provided by National Science Foundation awards OCE-1921654 and OCE-1801036 and NASA-80NSSC19M0069.

IX. References

Aluwihare, L. I., Repeta, D. J. and Chen, R. F., 1997. A major biopolymeric component to dissolved organic carbon in surface sea water. Nature, 387(6629), pp. 166-169.

Amend, J.P. and Shock, E.L., 1998. Energetics of Amino Acid Synthesis in Hydrothermal Ecosystems. Science 281: 1659-1662

Amend, J.P. and Shock, E.L., 2001. Energetics of overall metabolic reactions of the hyperthermophilic Archaea and Bacteria. FEMS Microbiology Reviews 25: 175-243

Amend, J. P., McCollom, T. M., Hentscher, M. and Bach, W., 2011. Catabolic and anabolic energy for chemolithoautotrophs in deep-sea hydrothermal systems hosted in different rock types. Geochim. Cosmochim. Acta 75(19), pp. 5736-5748.

Anantharaman, K., Breier, J.A., and Dick, G.J. 2016. Metagenoimic resolution of microbial functions in deep-sea hydrothermal plumes across the Eastern Lau Spreading Center. ISME Journal 10(1)225-239

Anderson, R.E., Brazelton. W.J., and Baross, J.A. 2013. The Deep Viriosphere: Assessing the Viral Impact on Microbial Community Dynamics in the Deep Subsurface. 75, pp. 649-675 In: Carbon in Earth (Ed: Hazen, R.M., Jones, A.P., Baross, J.A.) DOI: 2138/rmg.2013.75.20

Arakawa, N., Aluwihare, L. I., Simpson, A. J., Soong, R., Stephens, B. M. and Lane-Coplen, D. 2017. 'Carotenoids are the likely precursor of a significant fraction of marine dissolved organic matter. Sci. Adv. 3(9).

Aubrey, A., Cleaves, H. and Bada, J. 2009. The Role of Submarine Hydrothermal Systems in the Synthesis of Amino Acids. Orig. Life Evol. Biosph. 39(2), pp. 91-108.

Bemis, K., Lowell, R. P. and Farough, A. 2012. Diffuse Flow On and Around Hydrothermal Vents at Mid-Ocean Ridges. Oceanography 25(1), pp. 182-191.

Bennett, S. A., Achterberg, E. P., Connelly, D. P., Statham, P. J., Fones, G. R., & German, C. R. 2008. The distribution and stabilisation of dissolved Fe in deep-sea hydrothermal plumes. EPSL 270(3-4), 157-167. https://doi.org/10.1016/j.epsl.2008.01.048

Bennett, S. A., Statham, P. J., Green, D. R. H., Le Bris, N., McDermott, J. M., Prado, F., . . . German, C. R. 2011. Dissolved and particulate organic carbon in hydrothermal plumes from the East Pacific Rise, 9 degrees 50 ' N Deep-Sea Res. Part I Oceanogr. Res. Pap. 58(9), 922-931. https://doi.org/10.1016/j.dsr.2011.06.010

Bradley, A., Hayes, J. and Summons, R. (2009) 'Extraordinary C-13 enrichment of diether lipids at the Lost City Hydrothermal Field indicates a carbon-limited ecosystem', Geochim. Cosmochim. Acta , 73(1), pp. 102-118.

Breier, J. A., Toner, B. M., Fakra, S. C., Marcus, M. A., White, S. N., Thurnherr, A. M., & German, C. R. .2012. Sulfur, sulfides, oxides and organic matter aggregated in submarine hydrothermal plumes at 9 degrees 50 ' N East Pacific Rise. Geochim. Cosmochim. Acta , 88, 216-236. https://doi.org/10.1016/j.gca.2012.04.003

Canales, J. P., Dunn, R. A., Arai, R. and Sohn, R. A. 2017. Seismic imaging of magma sills beneath an ultramafic-hosted hydrothermal system. Geology, 45(5), pp. 451-454.

Carlson, C. A. and Hansell, D.A. 2015. DOM Sources, Sinks, Reactivity, and Budgets', in Hansell, D.A. & Carlson, C.A. (ed.) Biogeochemistry of Marine Dissolved Organic Matter: Academic Press, pp. 65-126.

Charlou, J. L., Donval, J. P., Fouquet, Y., Jean-Baptiste, P. and Holm, N. 2002. Geochemistry of high H(2) and CH(4) vent fluids issuing from ultramafic rocks at the Rainbow hydrothermal field (36 degrees 14 ' N, MAR). Chem. Geol. 191(4), pp. 345-359.

Coward, E. K., Ohno, T. and Plante, A. F. 2018. Adsorption and Molecular Fractionation of Dissolved Organic Matter on Iron-Bearing Mineral Matrices of Varying Crystallinity', Environ. Sci. Technol. 52(3), pp. 1036-1044.

Cruse, A. M. and Seewald, J. S. 2006. Geochemistry of low-molecular weight hydrocarbons in hydrothermal fluids from Middle Valley, northern Juan de Fuca Ridge. Geochim. Cosmochim. Acta 70(8), pp. 2073-2092.

de Ronde, C. E. J. and Stucker, V. K. 2015. Chapter 47 – Seafloor Hydrothermal Venting at Volcanic Arcs and Backarcs. Encyclopedia of Volcanoes, 2nd Ed.: Academic Press, pp. 823-849.

de Angelis, M. A., Lilley, M. D., Olson, E. J., & Baross, J. A. 1993. Methane oxidation in deep-sea hydrothermal plumes of the Endeavour segment of the Juan de Fuca Ridge. Deep-Sea Res. Part I Oceanogr. Res. Pap. 40(6), 1169-1186. https://doi.org/10.1016/0967-0637(93)90132-m

Dick, G. J. 2019. The microbiomes of deep-sea hydrothermal vents: distributed globally, shaped locally. Nat. Rev. Microbiol. 17(5), pp. 271-283.

Didyk, B. M. and Simoneit, B. R. T. 1989. Hydrothermal oil of Guaymas Basin and implications for petroleum formations. Nature, 342(6245), pp. 65-69.

Dittmar, T. and Koch, B. P. 2006. Thermogenic organic matter dissolved in the abyssal ocean. Mar. Chem. 102(3-4), pp. 208-217.

Druffel, E. R. M., Griffin, S., Lewis, C. B., Rudresh, M., Garcia, N. G., Key, R. M., McNichol, A. P., Hauksson, N. E. and Walker, B. D. 2021. Dissolved Organic Radiocarbon in the Eastern Pacific and Southern Oceans. Geophy. Res. Lett. 48(10).

Druffel, E.R.M., Griffin, S., Coppola, A.I., and Walker, B.D. 2016. Radiocarbon in dissolved organic carbon of the Atlantic Ocean' Geophy. Res. Lett. 43: 5279-5286

Druffel, E. R. M., Williams, P. M., Bauer, J. E. and Ertel, J. R. 1992. Cycling of dissolved and particulate organic matter in the open ocean', J. Geophys. Res. -Oceans, 97(C10), pp. 15639-15659.

Edwards, K. J., Bach, W. and McCollom, T. M. 2005. Geomicrobiology in oceanography: microbe-mineral interactions at and below the seafloor', Trends Microbiol. 13(9), pp. 449-456.

Edwards, K. J., Fisher, A. T. and Wheat, C. G. 2012. The deep subsurface biosphere in igneous ocean crust: frontier habitats for microbiological exploration. Front. Microbiol. 3.

Eglinton, T. I., Curtis, C. D. and Rowland, S. J. 1987. Generation of water soluble organic acids from kerogen during hydrous pyrolysis – implications for porosity development', Mineral. Mag. 51(362), pp. 495-503.

Eickenbusch, P., Takai, K., Sissman, O., Suzuki, S., Menzies, C., Sakai, S., Sansjofre, P., Tasumi, E., Bernasconi, S. M., Glombitza, C., Jorgensen, B. B., Morono, Y. and Lever, M. A. 2019. Origin of Short-Chain Organic Acids in Serpentinite Mud Volcanoes of the Mariana Convergent Margin', Front. Microbiol. 10.

Elderfield, H. and Schultz, A. 1996. Mid-ocean ridge hydrothermal fluxes and the chemical composition of the ocean. Annu. Rev. Earth Planet. 24, pp. 191-224.

Elderfield, H., Wheat, C. G., Mottl, M. J., Monnin, C. and Spiro, B. 1999. Fluid and geochemical transport through oceanic crust: a transect across the eastern flank of the Juan de Fuca Ridge. EPSL 172(1-2), pp. 151-165.

Emerson, D. and Moyer, C. L. 2002. Neutrophilic Fe-Oxidizing bacteria are abundant at the Loihi Seamount hydrothermal vents and play a major role in Fe oxide deposition. AEM 68(6), pp. 3085-3093.

Estes, E. R., Berti, D., Coffey, N. R., Hochella, M. F., Wozniak, A. S. and Luther, G. W. 2019. Abiotic synthesis of graphite in hydrothermal vents. Nat. Comm. 10.

Fisher, A. T. 2005. Marine hydrogeology: recent accomplishments and future opportunities', Hydrogeol. J. 13(1), pp. 69-97.

Fisher, A. T. and Wheat, C. G. 2010. Seamounts as Conduits for Massive Fluid, Heat, and Solute Fluxes on Ridge Flanks. Oceanography, 23(1), pp. 74-87.

Fisher, J. B. 1987. Distribution and occurrence of aliphatic acid anions in deep subsurface waters', Geochim. Cosmochim. Acta 51(9), pp. 2459-2468.

Fitzsimmons, J. N., Boyle, E. A. and Jenkins, W. J. 2014. Distal transport of dissolved hydrothermal iron in the deep South Pacific Ocean. PNAS 111(47), pp. 16654-16661.

Früh-Green, G. L., Kelley, D. S., Lilley, M. D., Cannat, M., Chavagnac, V. and Baross, J. A. 2022. Diversity of magmatism, hydrothermal processes and microbial interactions at mid-ocean ridges. Nat. Rev. Earth Environ. 3(12), pp. 852-871.

Frost, B. R. and Beard, J. S. 2007. On silica activity and serpentinization', Journal of Petrology, 48(7), pp. 1351-1368.

Fryer, P. 2012. Serpentinite Mud Volcanism: Observations, Processes, and Implications. Ann. Rev. Mar. Sci. Vol 4, 4, pp. 345-+.

Gelwicks, J.T., Risatti, J.B., and Hayes, J.M. 1994. Carbon Isotope Effects Associated with Aceticlastic Methanogenesis. Appl. Environ. Microbiol. 60(2): 467-472.

German, C.R. and Von Damm, K.L. 2003. 'Hydrothermal Processes', In H.D. Holland & K.K. Turekian (Eds.), Treatise on Geochemistry, First Edition (Vol. 6, pp. 181-222)

German, C. R., & Seyfried, W. E. 2014. 'Hydrothermal Processes', In H. D. Holland & K. K. Turekian (Eds.), Treatise on Geochemistry, Second Edition (Vol. 8, pp. 191-233).

German, C.R., Lang, S.Q., and Fitzsimmons, J.N. (in press) Hydrothermal Processes, In A. Paytan (Ed.), Treatise on Geochemistry, Third Edition

Gieskes, J. M., Simoneit, B. R. T., Goodfellow, W. D., Baker, P. A. and Mahn, C. 2002. Hydrothermal geochemistry of sediments and pore waters in Escanaba Trough - ODP Leg 169', Appl. Geochem. 17(11), pp. 1435-1456.

Giggenbach, W. F. 1984. Mass transfer in hydrothermal alteration systems – a conceptual approach. Geochim. Cosmochim. Acta , 48(12), pp. 2693-2711.

Glazer, B. T. and Rouxel, O. J. 2009. Redox Speciation and Distribution within Diverse Iron-dominated Microbial Habitats at Loihi Seamount Geomicrobiol. J. 26(8), pp. 606-622.

Glein, C.R., Gould, I.R., Lorance, E.D., Hartnett, H.E., and Shock 2020. Mechanisms of decarboxylation of phenylacetic acids and their sodium salts in water at high temperature and pressure. Geochim. Cosmochim. Acta, 269, pp. 597 - 621

Haberstroh, P. R. and Karl, D. M. 1989. Dissolved free amino-acids in hydrothermal vent habitats of the Guaymas Basin', Geochim. Cosmochim. Acta 53(11), pp. 2937-2945.

Haggerty, J. A. and Fisher, J. B. 1992. Short-chain organic acids in interstitial waters from forearc serpentines: Leg 125', in Fryer, P., Pearce, J.A., Stokking, L.B., et al. (ed.) Proc. Ocean Drill. Prog., Sci. results

Hawkes, J. A., Hansen, C. T., Goldhammer, T., Bach, W. and Dittmar, T. 2016. Molecular alteration of marine dissolved organic matter under experimental hydrothermal conditions. Geochim. Cosmochim. Acta , 175, pp. 68-85.

Hawkes, J. A., Rossel, P. E., Stubbins, A., Butterfield, D., Connelly, D. P., Achterberg, E. P., Koschinsky, A., Chavagnac, V., Hansen, C. T., Bach, W. and Dittmar, T. 2015. Efficient removal of recalcitrant deep-ocean dissolved organic matter during hydrothermal circulation. Nat. Geosci. 8(11), pp. 856-+.

Hedges, J. I. and Keil, R. G. 1995. Sedimentary organic matter preservation - an assessment and speculative synthesis', Mar. Chem. 49(2-3), pp. 81-115.

Hennet, R. J. C., Holm, N. G. and Engel, M. H. 1992. Abiotic synthesis of amino acids under hydrothermal conditions and the origin of life – a perpetual phenomenon. Sci. Nat. 79(8), pp. 361-365.

Hertkorn, N., Benner, R., Frommberger, M., Schmitt-Kopplin, P., Witt, M., Kaiser, K., Kettrup, A. and Hedges, J. I. 2006. Characterization of a major refractory component of marine dissolved organic matter', Geochim. Cosmochim. Acta , 70(12), pp. 2990-3010.

House, C.H., Schopf, J.W. and Stetter, K.O. 2003. Carbon isotopic fractionation by Archaeans and other thermophilic prokaryotes. Org. Geochem. 34: 345-356

Hu, S. R. K., Herrera, E. L., Smith, A. R., Pachiadaki, M. G., Edgcomb, V. P., Sylva, S. P., Chan, E. W., Seewald, J. S., German, C. R. and Huber, J. A. 2021. Protistan grazing impacts microbial communities and carbon cycling at deep-sea hydrothermal vents. PNAS 118(29).

Huber, J. A., Butterfield, D. A. and Baross, J. A. 2003. Bacterial diversity in a subseafloor habitat following a deep-sea volcanic eruption. Fems Microbiol. Ecol. 43(3), pp. 393-409.

Hunt, J. M. 1979. Petroleum Geochemistry and Geology. San Francisco: W.H. Freeman and Company.

Jenkins, W. J., Hatta, M., Fitzsimmons, J. N., Schlitzer, R., Lanning, N. T., Shiller, A., Buckley, N. R., German, C. R., Lott, D. E., Weiss, G., Whitmore, L., Casciotti, K., Lam, P. J., Cutter, G. A. and Cahill, K. L. 2020. An intermediate-depth source of hydrothermal He-3 and dissolved iron in the North Pacific. EPSL 539.

Johnson, H. P. and Pruis, M. J. 2003. Fluxes of fluid and heat from the oceanic crustal reservoir. EPSL 216(4), pp. 565-574.

Johnson-Finn, K.N., Gould, I.R., Williams, L.B., Hartnett, H.E., and Shock, E.L. 2020. Kinetics and Mechanisms of Hydrothermal Ketonic Decarboxylation. ACS Earth Space Chem. 4, pp. 2082-2095

Johnson-Finn, K.N., Williams, L.B., Gould, I.R., Hartnett, H.E. and Shock, E.L. 2021. Hydrothermal One-Electron Oxidation of Carboxylic Acids in the Presence of Iron Oxide Minerals. ACS Earth Space Chem. 5, pp. 2715-2728

Kadko, D. C., Rosenberg, N. D., Lupton, J. E., Collier, R. W., & Lilley, M. D. 1990. Chemical-reaction rates and entrainment within the Endeavor ridge hydrothermal plume. EPSL 99(4), 315-335.

Kaiser, K. and Guggenberger, G. 2000. The role of DOM sorption to mineral surfaces in the preservation of organic matter in soils Org. Geochem. 31(7-8), pp. 711-725.

Kawamura, K., Tannenbaum, E., Huizinga, B. J. and Kaplan, I. R. 1986. Volatile organic acids generated from kerogen during laboratory heating. Geochem. J. 20(1), pp. 51-59.

Kawka, O. E. and Simoneit, B. R. T. 1987. Survey of hydrothermally generated petroleum from Guaymas Basin spreading center. Org. Geochem. 11(4), pp. 311-328.

Keil, R. G., Hu, F. S., Tsamakis, E. C. and Hedges, J. I. 1994. Pollen in marine sediments as an indicator of oxidation of organic matter. Nature 369(6482), pp. 639-641.

Kelley, D. S., Karson, J. A., Fruh-Green, G. L., Yoerger, D. R., Shank, T. M., Butterfield, D. A., Hayes, J. M., Schrenk, M. O., Olson, E. J., Proskurowski, G., Jakuba, M., Bradley, A., Larson, B., Ludwig, K., Glickson, D., Buckman, K., Bradley, A. S., Brazelton, W. J., Roe, K., Elend, M. J., Delacour, A., Bernasconi, S. M., Lilley, M. D., Baross, J. A., Summons, R. T. and Sylva, S. P. 2005. A serpentinite-hosted ecosystem: The lost city hydrothermal field. Science 307(5714), pp. 1428-1434.

Konn, C., Charlou, J. L., Donval, J. P., Holm, N. G., Dehairs, F. and Bouillon, S. 2009. Hydrocarbons and oxidized organic compounds in hydrothermal fluids from Rainbow and Lost City ultramafic-hosted vents. Chem. Geol. 258(3-4), pp. 299-314.

Konn, C., Donval, J. P., Guyader, V., Germain, Y., Alix, A. S., Roussel, E. and Rouxel, O. 2022. Extending the dataset of fluid geochemistry of the Menez Gwen, Lucky Strike, Rainbow, TAG and Snake Pit hydrothermal vent fields: Investigation of temporal stability and organic contribution. Deep-Sea Res. Part I Oceanogr. Res. Pap. 179.

Kujawinski, E. B., Longnecker, K., Blough, N. V., Del Vecchio, R., Finlay, L., Kitner, J. B. and Giovannoni, S. J. 2009. Identification of possible source markers in marine dissolved organic matter using ultrahigh resolution mass spectrometry. Geochim. Cosmochim. Acta, 73(15), pp. 4384-4399.

Kvenvolden, K. A. 2006. Organic geochemistry - A retrospective of its first 70 years', Org. Geochem. 37(1), pp. 1-11.

Kvenvolden, K. A. and Simoneit, B. R. T. 1990. Hydrothermally derived petroleum – examples from Guaymas Basin, Gulf of California, and Escanaba Trough, Northeast Pacific Ocean. AAPG Bull. 74(3), pp. 223-237.

Lalonde, K., Mucci, A., Ouellet, A. and Gelinas, Y. 2012. Preservation of organic matter in sediments promoted by iron. Nature 483(7388), pp. 198-200.

Lam, P., Cowen, J. P., Popp, B. N., & Jones, R. D. 2008. Microbial ammonia oxidation and enhanced nitrogen cycling in the Endeavour hydrothermal plume. Geochim. Cosmochim. Acta 72(9), 2268-2286. https://doi.org/10.1016/j.gca.2008.01.033

Lang, S. Q. and Brazelton, W. J. 2020. Habitability of the marine serpentinite subsurface: a case study of the Lost City hydrothermal field. Philos. Trans. R. Soc. A. 378(2165).

Lang, S. Q., Butterfield, D. A., Lilley, M. D., Johnson, H. P. and Hedges, J. I. 2006. Dissolved organic carbon in ridge-axis and ridge-flank hydrothermal systems. Geochim. Cosmochim. Acta 70(15), pp. 3830-3842.

Lang, S. Q., Butterfield, D. A., Schulte, M., Kelley, D. S. and Lilley, M. D. 2010. Elevated concentrations of formate, acetate and dissolved organic carbon found at the Lost City hydrothermal field. Geochim. Cosmochim. Acta , 74(3), pp. 941-952.

Lang, S. Q., Fruh-Green, G. L., Bernasconi, S. M., Brazelton, W. J., Schrenk, M. O. and McGonigle, J. M. 2018. Deeply-sourced formate fuels sulfate reducers but not methanogens at Lost City hydrothermal field. Sci. Rep. 8.

Lang, S. Q., Fruh-Green, G. L., Bernasconi, S. M. and Butterfield, D. A. 2013. Sources of organic nitrogen at the serpentinite-hosted Lost City hydrothermal field. Geobiology 11(2), pp. 154-169.

Le Bris, N., Yucel, M., Das, A., Sievert, S. M., LokaBharathi, P. and Girguis, P. R. 2019. Hydrothermal Energy Transfer and Organic Carbon Production at the Deep Seafloor. Front. Mar. Sci. 5.

Li, J. T., Mara, P., Schubotz, F., Sylvan, J. B., Burgaud, G., Klein, F., Beaudoin, D., Wee, S. Y., Dick, H. J. B., Lott, S., Cox, R., Meyer, L. A. E., Quemener, M., Blackman, D. K. and Edgcomb, V. P. 2020. Recycling and metabolic flexibility dictate life in the lower oceanic crust. Nature 579(7798), pp. 250-+.

Lin, H. T., Amend, J. P., LaRowe, D. E., Bingham, J. P. and Cowen, J. P. 2015. Dissolved amino acids in oceanic basaltic basement fluids. Geochim. Cosmochim. Acta , 164, pp. 175-190.

Lin, H. T., Butterfield, D. A., Baker, E. T., Resing, J. A., Huber, J. A. and Cowen, J. P. 2021. Organic Biogeochemistry in West Mata, NE Lau Hydrothermal Vent Fields', Geochem. Geophys. Geosyst. 22(4).

Lin, H. T., Cowen, J. P., Olson, E. J., Amend, J. P. and Lilley, M. D. 2012. Inorganic chemistry, gas compositions and dissolved organic carbon in fluids from sedimented young basaltic crust on the Juan de Fuca Ridge flanks. Geochim. Cosmochim. Acta 85, pp. 213-227.

Lin, H. T., Repeta, D. J., Xu, L. and Rappe, M. S. 2019. Dissolved organic carbon in basalt-hosted deep subseafloor fluids of the Juan de Fuca Ridge flank. EPSL 513, pp. 156-165.

Lin, Y., Koch, B., Feseker, T., Ziervogel, K., Goldhammer, T., Schmidt, F., Witt, M., Kellermann, M., Zabel, M., Teske, A. and Hinrichs, K. 2017. Near-surface Heating of Young Rift Sediment Causes Mass Production and Discharge of Reactive Dissolved Organic Matter. Sci. Report. 7.

Longnecker, K., Sievert, S. M., Sylva, S. P., Seewald, J. S. and Kujawinski, E. B. 2018. Dissolved organic carbon compounds in deep-sea hydrothermal vent fluids from the East Pacific Rise at 9 degrees 50 ' N. Org. Geochem. 125, pp. 41-49.

Lough, A. J. M., Connelly, D. P., Homoky, W. B., Hawkes, J. A., Chavagnac, V., Castillo, A., Kazemian, M., Nakamura, K., Araki, T., Kaulich, B. and Mills, R. A. 2019. Diffuse Hydrothermal Venting: A Hidden Source of Iron to the Oceans. Front. Mar. Sci. 6.

Lundegard, P. D. and Kharaka, Y. K. 1994. Distribution and Occurrence of Organic Acids in Subsurface Waters. Berlin: Springer.

Lupton, J. E. and Craig, H. 1981. A major He-3 source at 15-degrees-S on the East Pacific Rise. Science, 214(4516), pp. 13-18.

Mason, O. U., Nakagawa, T., Rosner, M., Van Nostrand, J. D., Zhou, J. Z., Maruyama, A., Fisk, M. R. and Giovannoni, S. J. 2010. First Investigation of the Microbiology of the Deepest Layer of Ocean Crust. PLOS One, 5(11), pp. 11.

McCarthy, M., Beaupre, S., Walker, B., Voparil, I., Guilderson, T. and Druffel, E. 2011. Chemosynthetic origin of C-14-depleted dissolved organic matter in a ridge-flank hydrothermal system. Nat. Geosci. 4(1), pp. 32-36.

McCollom, T. M. 2000. Geochemical constraints on primary productivity in submarine hydrothermal vent plumes. Deep-Sea Res. Part I Oceanogr. Res. Pap. 47(1), pp. 85-101.

McCollom, T.M. and Seewald, J.S. 2001. A reassessment of the potential for reduction of dissolved CO_2 during serpentinization of olivine. Geochim. Cosmochim. Acta 65(21): 3769-3778

McCollom, T. M. and Seewald, J. S. 2007. Abiotic synthesis of organic compounds in deep-sea hydrothermal environments. Chem. Rev. 107(2), pp. 382-401.

McCollom, T. M., Seewald, J. S. and German, C. R. 2015. Investigation of extractable organic compounds in deep-sea hydrothermal vent fluids along the Mid-Atlantic Ridge. Geochim. Cosmochim. Acta 156, pp. 122-144.

McCollom, T. M., Seewald, J. S. and Simoneit, B. R. T. 2001. Reactivity of monocyclic aromatic compounds under hydrothermal conditions. Geochim. Cosmochim. Acta 65(3), pp. 455-468.

McCollom, T. M. and Shock, E. L. 1997. Geochemical constraints on chemolithoautotrophic metabolism by microorganisms in seafloor hydrothermal systems. Geochim. Cosmochim. Acta 61(20), pp. 4375-4391.

McDermott, J. M., Seewald, J. S., German, C. R. and Sylva, S. P. 2015. Pathways for abiotic organic synthesis at submarine hydrothermal fields. PNAS 112(25), pp. 7668-7672.

McKay, L. J., MacGregor, B. J., Biddle, J. F., Albert, D. B., Mendlovitz, H. P., Hoer, D. R., Lipp, J. S., Lloyd, K. G. and Teske, A. P. 2012. Spatial heterogeneity and underlying geochemistry of phylogenetically diverse orange and white Beggiatoa mats in Guaymas Basin hydrothermal sediments. Deep-Sea Res. Part I Oceanogr. Res. Papers 67, pp. 21-31.

Ménez, B., Pisapia, C., Andreani, M., Jamme, F., Vanbellingen, Q. P., Brunelle, A., Richard, L., Dumas, P. and Refregiers, M. 2018. Abiotic synthesis of amino acids in the recesses of the oceanic lithosphere. Nature 564(7734), pp. 59-+.

Michard, A., Michard, G., Stuben, D., Stoffers, P., Cheminee, J. L. and Binard, N. 1993. Submarine thermal springs associated with young volcanos – the Teahitia Vents, Society Islands, Pacific Ocean. Geochim. Cosmochim. Acta 57(21-22), pp. 4977-4986.

Moore, O.W., Curt, L., Woulds, C., Bradley, J.A., Babkhani, P., Mills, B.J.W., Homoky, W.B., Xiao, K.-Q., Bray, A.W., Fisher, B.J., Kazemian, M., Kaulich, B., Dale, A.W., and Peacok, C.L. 2023. Long-term organic carbon preservation enhanced by iron and manganese. Nature 621: 312-317

Mottl, M. J. 2003. Partitioning of Energy and Mass Fluxes between Mid-ocean Ridge Axes and Flanks at High and Low Temperature. Energy and Mass Transfer in Marine Hydrothermal Systems. Berlin: Dahlem University Press.

Mottl, M. J., McCollom, T. M., Wheat, G. and Fryer, P. 2023. Chemistry of springs across the Mariana forearc: Carbon flux from the subducting plate triggered by the lawsonite-to-epidote transition? Geochim. Cosmochim. Acta 340, pp. 1-20.

Mottl, M. J. and Wheat, C. G. 1994. Hydrothermal circulation through midocean ridge flanks - fluxes of heat and magnesium. Geochim. Cosmochim. Acta 58(10), pp. 2225-2237.

Mottl, M. J., Wheat, C. G., Fryer, P., Gharib, J. and Martin, J. B. 2004. Chemistry of springs across the Mariana forearc shows progressive devolatilization of the subducting plate. Geochim. Cosmochim. Acta 68(23), pp. 4915-4933.

Mottl, M. J., Wheat, G., Baker, E., Becker, N., Davis, E., Feely, R., Grehan, A., Kadko, D., Lilley, M., Massoth, G., Moyer, C. and Sansone, F. 1998. Warm springs discovered on 3.5 Ma oceanic crust, eastern flank of the Juan de Fuca Ridge. Geology 26(1), pp. 51-54.

Muller, R.D., Mather, B., Dutkiewicz, Keller, T., Meredith, A., Gonzalez, C.M., Gorczyk, W., and Zahirovic, S. 2022. Evolution of Earth's tectonic carbon conveyor belt. Nature, 605:629-639.

Nguyen, T.B., Topçuoğlu, B.D., Holden, J.F., Lang, S.Q. 2020. Lower hydrogen flux leads to larger carbon isotopic fractionation of methane and biomarkers during hydrogenotrophic methanogenesis. Geochim. Cosmochim. Acta 271: 212-226

Orcutt, B. N., Sylvan, J. B., Knab, N. J. and Edwards, K. J. 2011. Microbial Ecology of the Dark Ocean above, at, and below the Seafloor. Microbiol. Mol. Bio. 75(2), pp. 361-+.

Oro, J., Kimball, A., Fritz, R. and Master, F. 1959. Amino acid synthesis from formaldehyde and hydroxylamine. Arch. Biochem. Biophys. 85(1), pp. 115-130.

Pearson, A., Seewald, J.S. and Eglinton, T.I. 2005. Bacterial incorporation of relict carbon in the hydrothermal environment of Guaymas Basin', Geochim. Cosmochim. Acta, 69(23), pp.5477-5486

Penning, H. and Conrad, R. 2006. Carbon isotope effects associated with mixed-acid fementation of saccharides by Clostridium papyrosolvens. Geochim. Cosmochim. Acta 70: 2283-2297

Plank, T., Kelley, K. A., Zimmer, M. M., Hauri, E. H. and Wallace, P. J. 2013. Why do mafic arc magmas contain similar to 4 wt% water on average? EPSL 364, pp. 168-179.

Proskurowski, G., Lilley, M. D., Seewald, J. S., Fruh-Green, G. L., Olson, E. J., Lupton, J. E., Sylva, S. P. and Kelley, D. S. 2008. Abiogenic hydrocarbon production at Lost City hydrothermal field. Science 319(5863), pp. 604-607.

Qian, Y. R., Engel, M. H., Macko, S. A., Carpenter, S. and Deming, J. W. 1993. Kinetics of peptide hydrolysis and amino-acid decomposition at high-temperature. Geochim. Cosmochim. Acta 57(14), pp. 3281-3293.

Reeves, E. P., McDermott, J. M. and Seewald, J. S. 2014. The origin of methanethiol in midocean ridge hydrothermal fluids. PNAS 111(15), pp. 5474-5479.

Resing, J. A., Sedwick, P. N., German, C. R., Jenkins, W. J., Moffett, J. W., Sohst, B. M. and Tagliabue, A. 2015. Basin-scale transport of hydrothermal dissolved metals across the South Pacific Ocean. Nature 523(7559), pp. 200-U140.

Reveillaud, J., Reddington, E., McDermott, J., Algar, C., Meyer, J. L., Sylva, S., Seewald, J., German, C. R. and Huber, J. A. 2016. Subseafloor microbial communities in hydrogen-rich vent fluids from hydrothermal systems along the Mid-Cayman Rise. Environ. Microbiol. 18(6), pp. 1970-1987.

Robinson, K.J., Fecteau, K.M., Gould, I.R., Hartnett, H.E., Williams, L.B., and Shock, E.J. 2020. Metastable equilibrium of substitution reactions among oxygen- and nitrogen-bearing organic compounds at hydrothermal conditions. Geochim. Cosmochim. Acta 272, pp. 93-104

Robinson, K.J., Bockisch, C., Gould, I.R., Liao, Y., Yang, Z., Glein, C.R., Shaver, G.D., Hartnett, H.E., Williams, L.B., and Shock, E.L. 2021. Quantifying the extent of amide and peptide bond synthesis across conditions relevant to geologic and planetary environments. Geochim. Cosmochim. Acta 300, pp. 318-332

Rossel, P. E., Stubbins, A., Hach, P. F. and Dittmar, T. 2015. Bioavailability and molecular composition of dissolved organic matter from a diffuse hydrothermal system. Mar. Chem. 177, pp. 257-266.

Rossel, P. E., Stubbins, A., Rebling, T., Koschinsky, A., Hawkes, J. A. and Dittmar, T. 2017. Thermally altered marine dissolved organic matter in hydrothermal fluids', Org. Geochem. 110, pp. 73-86.

Rubin, K.H., Soule, S.A., Chadwick Jr., W.W., Fornari, D.J., Clague, D.A., Embley, R.W., Baker, E.T., Perfit, M.R., Caress, D.W., and Dziak, R.P. 2012. Volcanic eruptions in the deep sea. Oceanography 25(1):142-157

Rushdi, A. I. and Simoneit, B. R. T. 2004. Condensation reactions and formation of amides, esters, and nitriles under hydrothermal conditions. Astrobiol. 4(2), pp. 211-224.

Sander, S. G. and Koschinsky, A. 2011. Metal flux from hydrothermal vents increased by organic complexation', Nat. Geosci. 4(3), pp. 145-150.

Schrenk, M.O., Huber, J.A., and Edwards, K.J. 2010. Microbial Provinces in the Subseafloor. Annu. Rev. Mar. Sci. 2:279-304.

Schultz, A., Delaney, J. R. and McDuff, R. E. 1992. On the partitioning of heat-flux between diffuse and point-source sea-floor venting. J. Geophys. Res. Sol. Earth 97(B9), pp. 12299-12314.

Seewald, J. S. 2001a. Aqueous geochemistry of low molecular weight hydrocarbons at elevated temperatures and pressures: Constraints from mineral buffered laboratory experiments. Geochim. Cosmochim. Acta 65(10), pp. 1641-1664.

Seewald, J.S. 2001b. Model for the origin of carboxylic acids in basinal brines', Geochim. Cosmochim. Acta 65(21): 3779-3789

Seewald, J.S., Zolotov, M.Y., and McCollom, T. 2006. Experimental investigation of single carbon compounds under hydrothermal conditions. Geochim. Cosmochim. Acta. 70(2): 446-460

Seewald, J. S., Seyfried, W. E. and Thornton, E. C. 1990. Organic-rich sediment alteration - an experimental and theoretical study at elevated temperatures and pressures. Appl. Geochem. 5, pp. 193-209.

Seewald, J.S. 1994. Evidence for metastable equilibrium between hydrocarbons under hydrothermal conditions. Nature 370(6487): 285-287

Shebl, M. A. and Surdam, R. C. 1996. Redox reactions in hydrocarbon clastic reservoirs: experimental validation of this mechanism for porosity enhancement. Chem. Geol. 132(1), pp. 103-117.

Shock, E. L. 1992. Stability of peptides in high-temperature aqueous solutions. Geochim. Cosmochim. Acta 56(9), pp. 3481-3491.

Shock, E. L. 1993. Hydrothermal dehydration of aqueous organic compounds. Geochim. Cosmochim. Acta 57(14), pp. 3341-3349.

Shock, E. L., Canovas, P., Yang, Z. M., Boyer, G., Johnson, K., Robinson, K., Fecteau, K., Windman, T. and Cox, A. 2013. Thermodynamics of Organic Transformations in Hydrothermal Fluids. Thermodynamics of Geothermal Fluids, 76, pp. 311-350.

Shock, E. L. and Schulte, M. D. 1998. Organic synthesis during fluid mixing in hydrothermal systems. J. Geophys. Res. Planet. 103(E12), pp. 28513-28527.

Shock, E.L., Bockisch, C., Estrada, C., Fecteau, K., Gould, I.R., Hartnett, H., Johnson, K., Robinson, K., Shipp, J., and Williams, L. 2019. Earth as Organic Chemist. In: Deep Carbon Past to Present, Orcutt, B.N., Daniel, I., Dasgupta, R., Eds; Cambridge University Press: Cambridge, 2010, pp 415-446

Simoneit, B. R. T. 1985. Hydrothermal petroleum – genesis, migration, and deposition in Guaymas Basin, Gulf of California. Can. J. Earth Sci. 22(12), pp. 1919-1929.

Simoneit, B. R. T. and Fetzer, J. C. 1996. High molecular weight polycyclic aromatic hydrocarbons in hydrothermal petroleums from the Gulf of California and Northeast Pacific Ocean. Org. Geochem. 24(10-11), pp. 1065-1077.

Simoneit, B. R. T., Kawka, O. E. and Brault, M. 1988. Origin of gases and condensates in the Guaymas Basin hydrothermal system (Gulf of California). Chem. Geol. 71(1-3), pp. 169-182.

Simoneit, B. R. T. and Lonsdale, P. F. 1982. Hydrothermal petroleum in mineralized mounds at the seabed of Guaymas Basin. Nature, 295(5846), pp. 198-202.

Staudigel, H., Hart, S. R., Koppers, A. A. P., Constable, C., Workman, R., Kurz, M. and Baker, E. T. 2004. 'Hydrothermal venting at Vailulu'u Seamount: The smoking end of the Samoan chain. Geochem. Geophys. Geosyst. 5.

Stein, C.A. and Stein, S. 1994. Constraints on hydrothermal heat flux through the oceanic lithosphere from global heat flow. J. Geophys. Res. 99(B2): 3081-3094

Summit, M. and Baross, J. A. 2001. A novel microbial habitat in the mid-ocean ridge subseafloor. PNAS 98(5), pp. 2158-2163.

Suzuki, Y., Yamashita, S., Kouduka, M., Ao, Y., Mukai, H., Mitsunobu, S., Kagi, H., D'Hondt, S., Inagaki, F., Morono, Y., Hoshino, T., Tomioka, N. and Ito, M. 2020. Deep microbial proliferation at the basalt interface in 33.5-104 million-year-old oceanic crust. Comm. Biol. 3(1).

Svensson, E., Skoog, A. and Amend, J. P. 2004. Concentration and distribution of dissolved amino acids in a shallow hydrothermal system, Vulcano Island (Italy). Org. Geochem. 35(9), pp. 1001-1014.

Tagliabue, A., Bopp, L., Dutay, J.-C., Bowie, A.R., Chever, F., Jean-Baptiste, P., Bucciarelli, E., Lannuzel, D., Remenyi, T., Sarthou, G., Aumont, O., Gehlen, M., and Jeandel, C. 2010. Hydrothermal contribution to the oceanic dissolved iron inventory. Nat. Geosci. 3:252-256

Teske, A., de Beer, D., McKay, L. J., Tivey, M. K., Biddle, J. F., Hoer, D., Lloyd, K. G., Lever, M. A., Roy, H., Albert, D. B., Mendlovitz, H. P. and MacGregor, B. J. 2016. The Guaymas Basin Hiking Guide to Hydrothermal Mounds, Chimneys, and Microbial Mats: Complex Seafloor Expressions of Subsurface Hydrothermal Circulation. Front. Microbiol. 7.

Tissot, B. P. and Welte, D. H. 1984. Petroleum Formation and Occurrence. Berlin: Springer.

Toner, B. M., Santelli, C. M., Marcus, M. A., Wirth, R., Chan, C. S., McCollom, T., . . . Edwards, K. J. 2009. ‘Biogenic iron oxyhydroxide formation at mid-ocean ridge hydrothermal vents: Juan de Fuca Ridge. Geochim. Cosmochim. Acta 73(2), 388-403. https://doi.org/10.1016/j.gca.2008.09.035

Treibs, A. 1936. Chlorophyll and heme derivatives in organic mineral materials. Angew Chem. 49, pp. 0682-0686.

Veirs, S. R., McDuff, R. E. and Stahr, F. R. 2006. Magnitude and variance of near-bottom horizontal heat flux at the Main Endeavour hydrothermal vent field. Geochem. Geophy. Geosyst. 7.

Villinger, H. W., Muller, P., Bach, W., Becker, K., Orcutt, B. N., Kaul, N. and Wheat, C. G. 2019. Evidence for Low-Temperature Diffuse Venting at North Pond, Western Flank of the Mid-Atlantic Ridge. Geochem. Geophys. Geosyst. 20(6), pp. 2572-2584.

Von Damm, K. L. and Lilley, M. D. 2004. Diffuse Flow Hydrothermal Fluids from 9-degrees 50' N East Pacific Rise: Origin, Evolution and Biogeochemical Controls. The Subseafloor Biosphere at Mid-Ocean Ridges, pp. 245-268.

Wagner, S., Brandes, J., Spencer, R. G. M., Ma, K., Rosengard, S. Z., Moura, J. M. S. and Stubbins, A. 2019. Isotopic composition of oceanic dissolved black carbon reveals non-riverine source. Nat. Comm. 10.

Wallace, P. J. 2005. Volatiles in subduction zone magmas: concentrations and fluxes based on melt inclusion and volcanic gas data. J. of Volcanol. Geotherm. Res. 140(1-3), pp. 217-240.

Walter, S. R. S., Jaekel, U., Osterholz, H., Fisher, A. T., Huber, J. A., Pearson, A., Dittmar, T. and Girguis, P. R. 2018. Microbial decomposition of marine dissolved organic matter in cool oceanic crust. Nat. Geosci. 11(5), pp. 334-+.

Wankel, S. D., Germanovich, L. N., Lilley, M. D., Genc, G., DiPerna, C. J., Bradley, A. S., Olson, E. J. and Girguis, P. R. 2011. Influence of subsurface biosphere on geochemical fluxes from diffuse hydrothermal fluids. Nat. Geosci. 4(7), pp. 461-468.

Wellsbury, P., Goodman, K., Barth, T., Cragg, B., Barnes, S. and Parkes, R. 1997. Deep marine biosphere fuelled by increasing organic matter availability during burial and heating. Nature, 388(6642), pp. 573-576.

Wheat, C. G., Feely, R. A. and Mottl, M. J. 1996. Phosphate removal by oceanic hydrothermal processes: An update of the phosphorus budget in the oceans. Geochim. Cosmochim. Acta 60(19), pp. 3593-3608.

Wheat, C. G. and Fisher, A. T. 2008. Massive, low-temperature hydrothermal flow from a basaltic outcrop on 23 Ma seafloor of the Cocos Plate: Chemical constraints and implications. Geochem. Geophys. Geosyst. 9.

Wheat, C. G., Hartwell, A. M., McManus, J., Fisher, A. T., Orcutt, B. N., Schlicht, L. E. M., Niedenzu, S. and Bach, W. 2019. Geology and Fluid Discharge at Dorado Outcrop, a Low Temperature Ridge-Flank Hydrothermal System. Geochem. Geophys. Geosyst. 20(1), pp. 487-504.

Wheat, C. G., Hulme, S. M., Fisher, A. T., Orcutt, B. N. and Becker, K. 2013. Seawater recharge into oceanic crust: IODP Exp 327 Site U1363 Grizzly Bare outcrop. Geochem. Geophys. Geosyst. 14(6), pp. 1957-1972.

Winn, C. D., Karl, D. M., & Massoth, G. J. 1986. Microorganisms in deep-sea hydrothermal plumes. Nature 320(6064), 744-746. https://doi.org/10.1038/320744a0

Yamashita, S., Mukai, H., Tomioka, N., Kagi, H. and Suzuki, Y. 2019. Iron-rich Smectite Formation in Subseafloor Basaltic Lava in Aged Oceanic Crust. Sci. Rep. 9.

Yamashita, Y., Nakane, M., Mori, Y., Nishioka, J. and Ogawa, H. 2022. Fate of dissolved black carbon in the deep Pacific Ocean. Nat. Comm. 13(1).

Yanagawa, H. and Kobayashi, K. 1992. An experimental approach to chemical evolution in submarine hydrothermal systems. Orig. Life Evol. Biosph. 22(1-4), pp. 147-159.

Yang, L. Y., Zhuang, W. E., Chen, C. T. A., Wang, B. J. and Kuo, F. W. 2017. Unveiling the transformation and bioavailability of dissolved organic matter in contrasting hydrothermal vents using fluorescence EEM-PARAFAC. Water Res. 111, pp. 195-203.

Zhuang, G. C., Montgomery, A., Samarkin, V. A., Song, M., Liu, J. R., Schubotz, F., Teske, A., Hinrichs, K. U. and Joye, S. B. 2019. Generation and Utilization of Volatile Fatty Acids and Alcohols in Hydrothermally Altered Sediments in the Guaymas Basin, Gulf of California. Geophys. Res. Lett. 46(5), pp. 2637-2646.

Ziolkowski, L. A. and Druffel, E. R. M. 2010. Aged black carbon identified in marine dissolved organic carbon. Geophys. Res. Lett. 37.

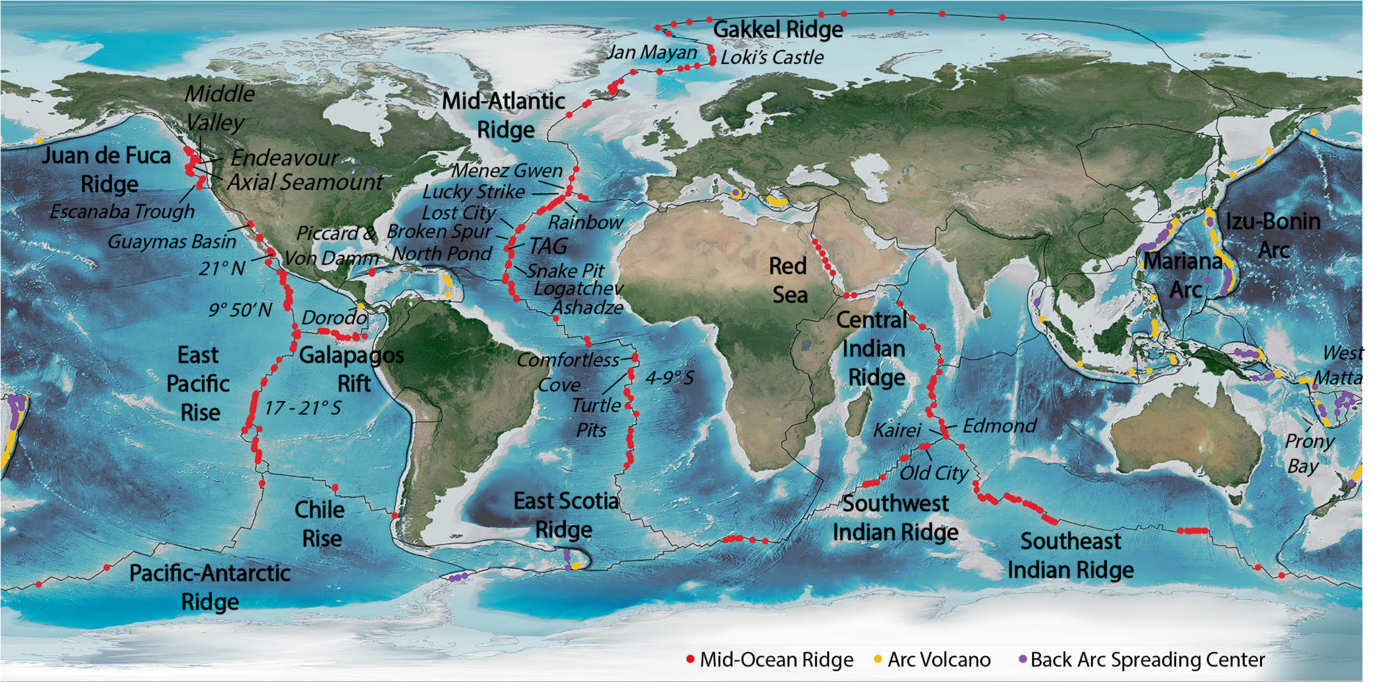
Gakkel Ridge
Jan Mayan
Loki's Castle
Middle Valley
Mid-Atlantic Ridge
Juan de Fuca Ridge
Endeavour
Axial Seamount
Escanaba Trough
Menez Gwen
Lucky Strike
Lost City
Rainbow
Guaymas Basin
Piccard & Von Damm
Broken Spur
TAG
North Pond
21° N
Snake Pit
Logatchev
Ashadze
9° 50′ N
Dorodo
Red Sea
Central Indian Ridge
Izu-Bonin Arc
Mariana Arc
East Pacific Rise
Galapagos Rift
Comfortless Cove
4-9° S
Turtle Pits
17 - 21° S
West Matta
Kairei
Edmond
Old City
Prony Bay
Chile Rise
East Scotia Ridge
Southwest Indian Ridge
Southeast Indian Ridge
Pacific-Antarctic Ridge
● Mid-Ocean Ridge
● Arc Volcano
● Back Arc Spreading Center

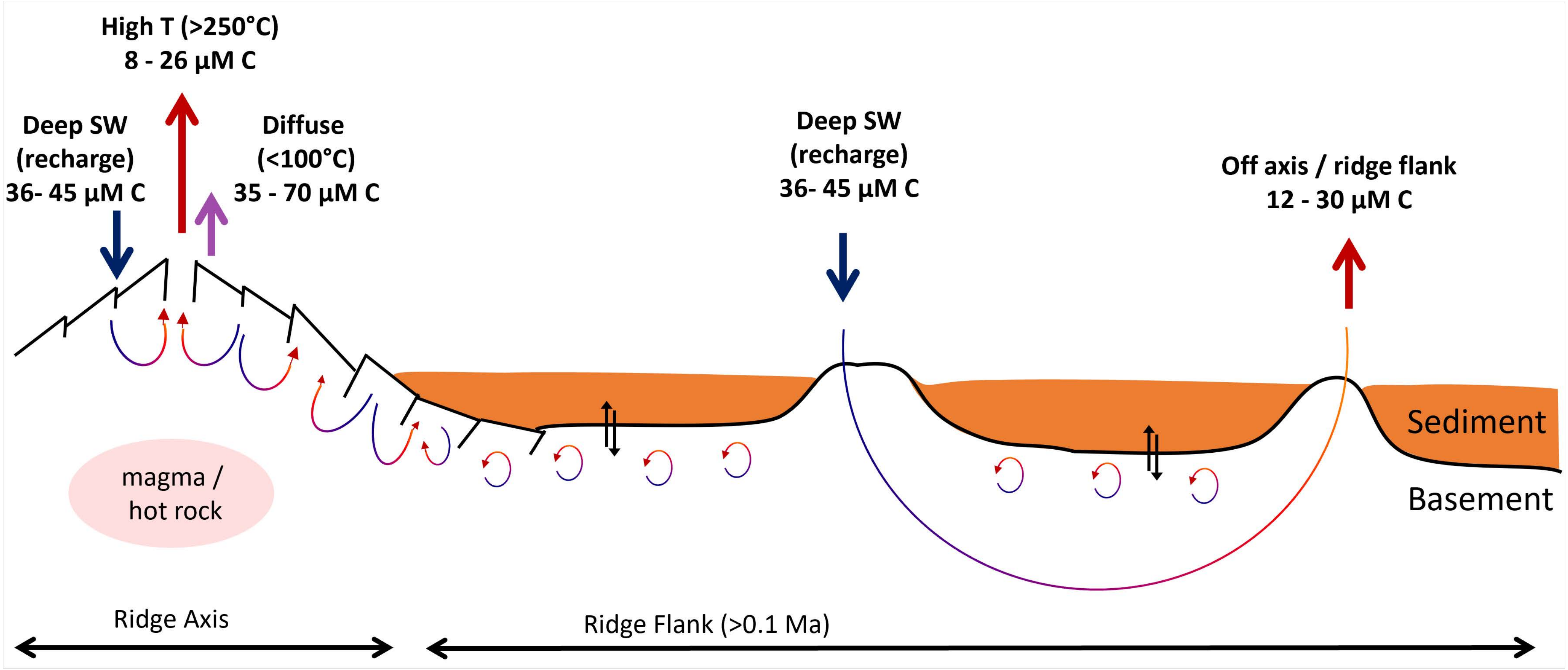
High T (>250°C)
8 - 26 µM C
Deep SW
(recharge)
36- 45 µM C
Diffuse
(<100°C)
35 - 70 µM C
Deep SW
(recharge)
36- 45 µM C
Off axis / ridge flank
12 - 30 µM C
Sediment
Basement
magma /
hot rock
Ridge Axis
Ridge Flank (>0.1 Ma)

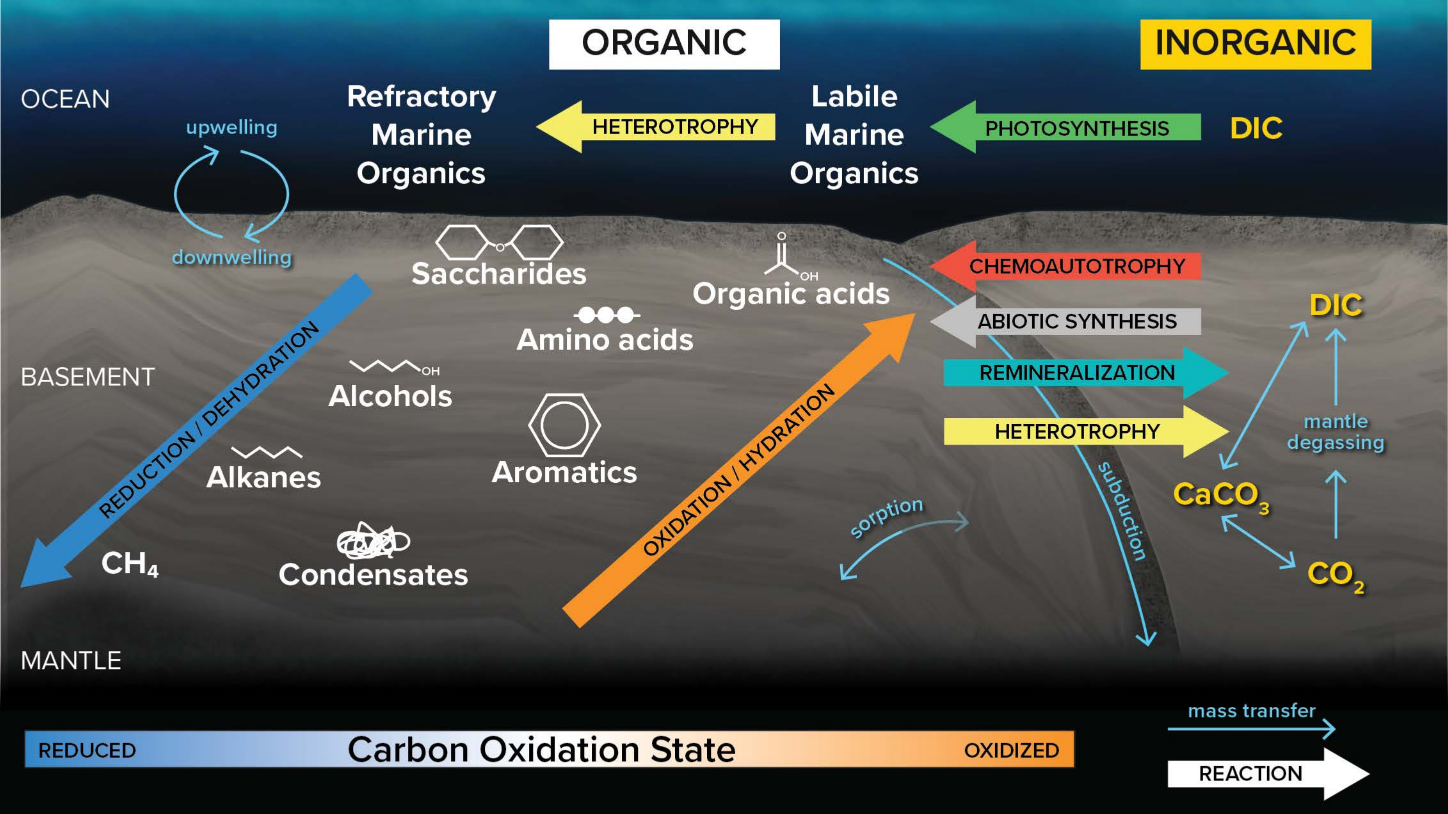
ORGANIC
INORGANIC
OCEAN
Refractory Marine Organics
HETEROTROPHY
Labile Marine Organics
PHOTOSYNTHESIS
DIC
upwelling
downwelling
Saccharides
O
O
OH
Organic acids
CHEMOAUTOTROPHY
ABIOTIC SYNTHESIS
DIC
Amino acids
REDUCTION / DEHYDRATION
BASEMENT
OH
Alcohols
REMINERALIZATION
HETEROTROPHY
mantle degassing
Aromatics
OXIDATION / HYDRATION
Alkanes
subduction
$CaCO_3$
sorption
CH_4
Condensates
CO_2
MANTLE
mass transfer
REDUCED
Carbon Oxidation State
OXIDIZED
REACTION

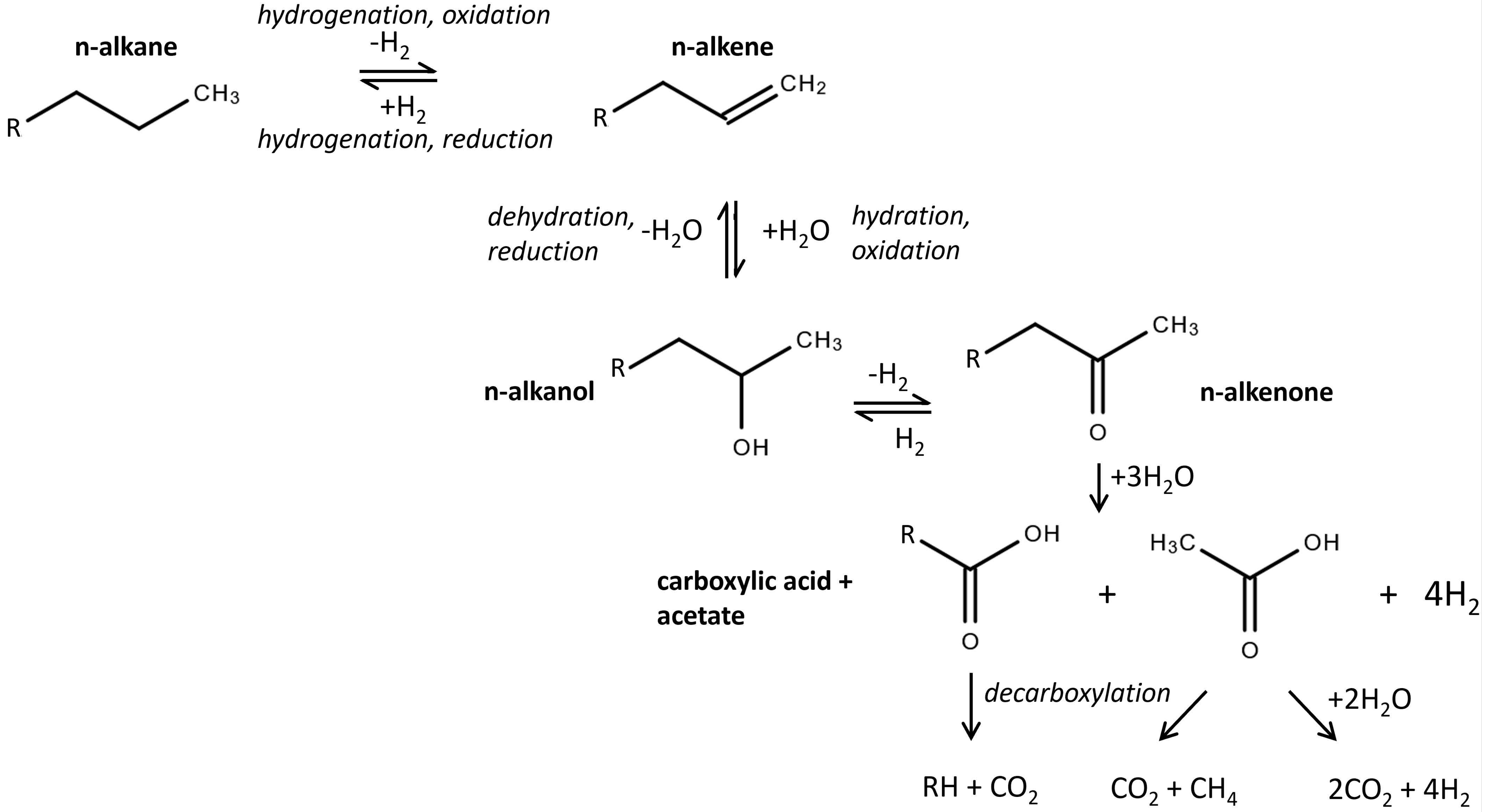
n-alkane
hydrogenation, oxidation
$-H_2$
$+H_2$
hydrogenation, reduction
n-alkene
dehydration, reduction
$-H_2O$
$+H_2O$
hydration, oxidation
n-alkanol
$-H_2$
H_2
n-alkenone
$+3H_2O$
carboxylic acid + acetate
$+ 4H_2$
decarboxylation
$+2H_2O$
$RH + CO_2$
$CO_2 + CH_4$
$2CO_2 + 4H_2$

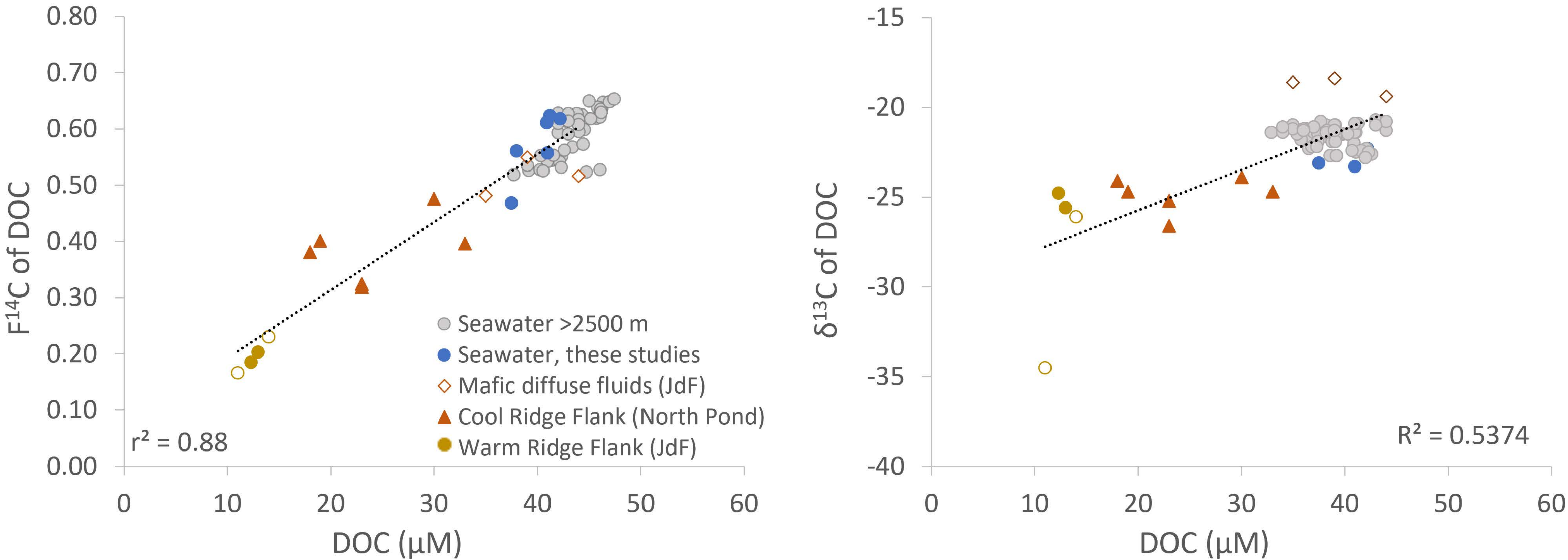
0.80
0.70
0.60
0.50
0.40
0.30
0.20
0.10
0.00
F^{14}C of DOC
0
10
20
30
40
50
60
DOC (µM)
r² = 0.88
Seawater >2500 m
Seawater, these studies
Mafic diffuse fluids (JdF)
Cool Ridge Flank (North Pond)
Warm Ridge Flank (JdF)
-15
-20
-25
-30
-35
-40
δ^{13}C of DOC
0
10
20
30
40
50
60
DOC (µM)
R² = 0.5374